Science of the Total Environment 986 (2025) 179700

Contents lists available at ScienceDirect

Science of the Total Environment

journal homepage: www.elsevier.com/locate/scitotenv

Contrasting growth responses in Himalayan trees to future climate

Rupesh Dhyani [a,e,1], Pablo Casas-Gómez [b,1], Lea Schneider [a,h], Raúl Sánchez-Salguero [b], Shinny Thakur [c,e], Mayank Shekhar [d], Rajesh Joshi [e], Jagdish Chandra Kuniyal [f], Amalava Bhattacharyya [d], Surendra Pratap Singh [g], Juan Carlos Linares [b,*]

[a] Department of Geography, Justus-Liebig-University, Giessen, Germany
[b] Departamento Sistemas Físicos, Químicos y Naturales, Universidad Pablo de Olavide, 41013 Sevilla, Spain
[c] Indian Council of Forestry Research and Education, Dehradun, India
[d] Birbal Sahni Institute of Palaeosciences, 53 University Road, Lucknow 226007, India
[e] Govind Ballabh Pant National Institute of Himalayan Environment (NIHE), Kosi-Katarmal, Almora 263 643, Uttarakhand, India
[f] Department of Forest Resource Management, College of Forestry, Veer Chandra Singh Garhwali Uttarakhand University of Horticulture and Forestry (VCSG UUHF), Ranichauri-249 199, Tehri Garhwal, Uttarakhand, India
[g] Central Himalayan Environment Association, Dehradun, India
[h] Center for international Development and Environmental Research, Justus-Liebig-University, Giessen, Germany

HIGHLIGHTS

- Himalayan trees show regional- and species-specific responses to future climate change.
- Growth declines in monsoon dominated regions are linked to higher evaporative demand.
- Westerly dominated trees benefit from increased winter precipitation.
- We recommend conserving eastward and adapting management westward.

GRAPHICAL ABSTRACT

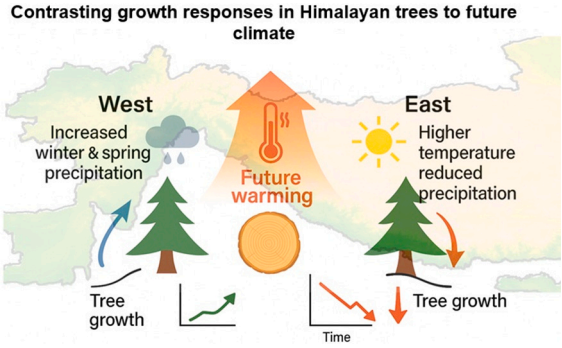

ARTICLE INFO

Editor: Manuel Esteban Lucas-Borja

Keywords:
Hindu-Kush Himalaya
Tree rings
Monsoon
Westerlies
Basal Area Increment
Future warming

ABSTRACT

Rising temperatures and shifting regional precipitation patterns are exerting significant impact on tree growth in the Himalayan region. Despite growing concern about global warming, the regional- and species-specific growth responses to future climate scenarios remain poorly quantified across the two contrasting precipitation regimes (Eastern-monsoon vs Western-westerly) of the Himalaya. We analyzed 3370 time series of tree-ring width data of 14 dominant tree species in the Himalaya occurring between 1750 and 4100 m of elevation covering a large longitudinal monsoon-related environmental gradient. With Linear Mixed Models (LMMs), we predicted Basal Area Increment (BAI) trends for different temperature and precipitation changes under four representative concertation pathways (RCP 2.6, 4.5, 6.0 and 8.5). Results show contrasting patterns: in the Eastern region, species such as *Cedrus deodara* and *Pinus roxburghii* are projected to decline by 23–67 % in BAI by the end of the

* Corresponding author.
E-mail address: jclincal@upo.es (J.C. Linares).
[1] Authors 1st and 2nd contributed equally to the manuscript.

https://doi.org/10.1016/j.scitotenv.2025.179700
Received 14 February 2025; Received in revised form 15 May 2025; Accepted 15 May 2025

21th century under all the climate scenarios due to warming-induced moisture stress. Conversely, in the Western region, species like *Picea smithiana* and *Pinus wallichiana* shows projected gain in BAI up 100 % likely due to enhanced winter and spring precipitation from westerlies. Likely increased forest carbon sequestration in selected species in the Western region highlights the importance of spatially targeted climate informed forest management. Our results evidence the need for conservation strategies in the Eastern region, while adaptive management should be considered in the Western region to maintain Himalayan forest resilience and sustainability in the face of future warming.

1. Introduction

Climate change is profoundly affecting forest ecosystems worldwide, particularly in mountainous regions where temperature and precipitation regimes are changing rapidly and heterogeneously. The accelerating pace of climate change is projected to markedly influence forest growth dynamics and alter their carbon sequestration potential. Understanding how forest species respond to these changes is critical for biodiversity conservation and the maintenance of vital ecosystem services (Allen et al., 2015).

Climate change affects growth in tree species depending on the interaction of multiple intrinsic (e.g. tree age) and extrinsic factors (Camarero et al., 2017; Matías et al., 2017; Shi et al., 2021a, 2021b) (e.g., regional climate, topography and soil moisture). Tree species adapted to high-elevation environments may have improved adaptive capacity to changing climate if they are able to perform altitudinal distribution shifts (Telwala et al., 2013; Camarero et al., 2017). However, those tree species already endangered by limited distribution ranges should be particularly vulnerable to ongoing climate change (Cuo et al., 2013; Liu et al., 2007; Manabe and Broccoli, 1990; Yanai et al., 1992).

This complexity is particularly pronounced in the Himalayan region, a global biodiversity hotspot and also known as the third pole, affects climate dynamics not only in Southeast Asia but also beyond its geographic limits (Sharma et al., 2019). The Himalayan forests play a crucial role in regional and global carbon dynamics acting as substantial carbon sinks through biomass accumulation and long-term carbon storage in soils. Forests dominated by major tree species in this region store an estimated 6–7 billion tons of carbon significantly contributing to national carbon budgets and climate mitigation goals. However, the future carbon sequestration potential of these forests remains uncertain as changes in tree growth rates or species composition may alter their ability to offset emissions.

Rapid warming has already been observed in several parts of the Himalaya (Krishnan et al., 2019; Sabin et al., 2020). In some areas, precipitation is decreasing, while average warming is expected to increase at least 0.3 °C overall the Himalayan region, although it is expected to rise up to 0.7 °C in the northwest Himalaya and Karakoram, where an increase in winter and spring precipitation driven by mid-latitude westerlies has also been observed in recent decades (Krishnan et al., 2019). Under these assumptions, a decrease in forests growth and declining distribution ranges might be expected for several tree species in response to warming and shifting precipitation regimes (Bhattacharyya et al., 2023; Chakraborty et al., 2016). In addition, the temperature increase, among the highest worldwide, implies more severe water stress for some already water-limited Himalayan forest ecosystems. Conversely, in some regions, warmer and wetter conditions have been observed, creating more favorable conditions for tree growth. In particular, the northwest Himalaya and Karakoram have experienced increased winter and spring precipitation driven by the mid-latitude westerlies which can mitigate water stress and support higher growth rates especially for moisture-sensitive tree species in the semi-arid zones (Shekhar et al., 2017; Yadav et al., 2017). The growth variability in these contrasting areas will largely depend on the continued interplay between temperature increases and precipitation patterns with wetter conditions potentially offsetting some of the negative impacts of warming on forest ecosystems.

From a regional point of view, the climate of the Himalaya is driven by monsoon and westerly winds, as large amounts of precipitation is brought by south westerly monsoon winds during the summer season (June–September) and westerly winds during the winter seasons (Krishnan et al., 2019). total rainfall decreases westward, increasing the regional aridity from the Eastern to the Western region. The distribution of tree species in the region is closely linked to the precipitation regimes (Singh et al., 2017). Monsoon-influenced regions support species that thrive in moist, warm conditions, while areas with significant winter precipitation support species adapted to cooler and drier environments.

The current state of Himalayan forests is precarious, with many dominant tree species showing reduced vitality (Thakur et al., 2021), increased mortality (Mainali et al., 2020), and slower regeneration (Kumar and Khanduri, 2024). Yet, not all projected climatic shifts result in negative consequences. For instance, dominant forest trees like firs (*Abies* spp.) are projected to decline, losing 6–14 % of their distribution area, mainly at the lower elevation range limits. However, potential increases are expected at their upper elevation range limits by an altitudinal migration of about 30 m per decade (Malik et al., 2022). Similarly, the dominant species *Cedrus deodara* is expected to gain its potential distribution in Western Himalaya but loss in distribution area in the Eastern region over the 21st century due to regional climate differences (Xiao et al., 2022). Recent tree-ring observations revel that under future climate scenarios, rising temperatures in the monsoon influenced Himalayan region are likely to intensify evapotranspiration, exacerbating moisture stress and leading to reduced tree growth, whereas in the westerly dominated region, increased winter precipitation is projected to provide additional moisture during the dry growing season supporting moderate growth increases under both climate (Bhattacharyya et al., 2023). As regional climate responds differently to global warming across the contrasting Himalaya region, co-occurring species will likely exhibit diverse growth patterns.

Tree ring width (TRW) data has been extensively used in the Himalayan region to reconstruct past climate variability (Dhyani et al., 2023; Dhyani et al., 2022a, 2022b; Shekhar and Bhattacharyya, 2015; Yadav et al., 2011 Cook et al., 2003). The annual increment in TRW reflects the outcome of dynamic ecological interactions with weather and inherent physiological patterns associated with tree age and structural size. Basal Area Increment (BAI) offers an advantage over raw tree-ring width measurements by incorporating the geometric expansion of a tree stem over time (Biondi and Qeadan, 2008). This method provides a more realistic approximation of wood production and biomass accumulation, because BAI compensates for this natural growth trend in TRW data enabling more accurate and comparable growth assessments across various tree ages and species (Bosela et al., 2023; Martinez del Castillo et al., 2022). Understanding how inherent characteristics of tree-growth patterns, such as species-specific growth rates, tree age-effects or forest stand respond to climatic variability is essential for interpreting growth outcomes across in the context of topographic and regional climatic gradients contribute meaningful to the growth outcomes (Anderson-Teixeira et al., 2022; Martinez del Castillo et al., 2022). Hence, some studies suggest that old trees are more sensitive to temperature, while younger trees rely more on short-term soil water availability (Delzon and Loustau, 2005; Knapp and Soulé, 2011; Li et al., 2013; Magnani et al., 2000; Ruiz-Benito et al., 2015; Ryan et al., 2006; Shi et al., 2021a, 2021b; Zeng et al., 2018). In addition, other studies

suggest that larger trees, that is, those accounting for greater carbon stock in their biomass, may be more sensitive to climate changes (Stephenson et al., 2014; McDowell et al., 2011). Understanding these size- and age-related growth sensitivities is particularly important when interpreting how climate variability interacts with topographic and regional climatic gradients (Klesse et al., 2020; Sánchez-Salguero et al., 2017a, 2017b).

Recent advancements in statistical modeling have expanded the utility of tree-ring data beyond historical reconstructions (Bosela et al., 2023; Klesse et al., 2020, 2024; Martinez del Castillo et al., 2022; Sánchez-Salguero et al., 2017a, 2017b). Linear mixed-effects models and other approaches now allow researchers to explore spatial and temporal growth variability and identify key climatic drivers (Anderson-Teixeira et al., 2022; Klesse et al., 2020, 2024; Martinez del Castillo et al., 2022). These models can simulate past and future growth patterns, often using space-for-time substitution and data-driven regressions to integrate species-specific climate sensitivity with environmental gradients. Incorporating tree-level variables, age and site characteristics these models can produce spatially explicit estimates comparable with other forest dynamics (Anderson-Teixeira et al., 2022; Klesse et al., 2024; Martinez del Castillo et al., 2022).

Here, we investigate tree-ring data from 14 major tree species of the Himalayan region to model growth patterns and predict growth trends under contrasting climate scenarios. Our specific aims are (i) to model the species-specific growth patterns of tree populations growing under two contrasting regional climates, namely, the Eastern region with monoon influence and the Western region influenced by westerlies (ii) to predict growth trends according to expected climate change scenarios (RCP 2.6, 4.5, 6.0, 8.5). We hypothesize that predicted increased temperature during the growing season would reduce the growth of trees in the monsoon dominated regions by a warming-induced water shortage. On the other hand, since the westerlies are predicted to become stronger due to climate change (Krishnan et al., 2019; Sabin et al., 2020), tree growth might be improved following increased winter and spring precipitation westward where the growing season typically lacks sufficient rainfall.

2. Materials and methods

2.1. Tree ring data

This study was carried out in the Hindu Kush Himalayan (HKH) region (Fig. 1) comprising cross-dated tree ring records of 14 species obtained from the International Tree-Ring Data Bank (ITRDB) from a total of 116 locations spanning latitudes 27.17°–36.61° N and longitudes 74.98°–86.42° E and elevation ranges between 1310 and 4100 m a.s.l. (Fig. 1). The sampled species are ecologically significant forming dominant forest types across the HKH region with well-defined distribution boundaries (Singh et al., 2017). Genus; *Abies*, *Picea*, and *Tsuga* predominantly occupy moist subalpine zones between 2800 and 3800 m, *Cedrus* and *Pinus* are widespread in dry mid high elevation forests ranging from 1500 to 3000 m (Singh and Zobel, 2025), and *Juniperus* and *Betula* are characteristic of high-altitude moist and arid regions extending from 3200 to 4500 m collectively covering substantial portions of the regional forest composition and structure from Western to Eastern region. Ranging from dry coniferous forests in the West to moisture-rich subalpine and alpine forests in the East, reflecting a gradient of increasing precipitation and climatic variability. To ensure ecological and climatic relevance, we selected sites with at least 50 years of tree ring data. These records were further screened for consistency in cross-dating and metadata quality. To assess the role of contrasting climatic regimes, we classified the sites into two broad sub-regions: Eastern and Western (Fig. 1). These Two regions were defined according to the percentage of annual rainfall during the monsoon season: in the East 70–80 % of annual precipitation is due to the monsoon and in the West the monsoon accounts for <50 % of annual precipitation together with considerable amounts of winter precipitation from the westerlies (Singh et al., 2017; Sabin et al., 2020). The Eastern region comprises a total of 71 populations, while the Western region provides the remaining 45 populations (Fig. 1). TRW data was converted into the Basal Area Increment (BAI) commonly used in tree growth modeling using the following equation:

$$BAI = \pi\left(R_t^2 - R_{t-1}^2\right) \quad (1)$$

where BAI is the basal area increment in the year *t*. R_t is the radius of the tree at year t and R_{t-1} is the radius of the tree at year t-1.

Outliers detection was performed on raw BAI data and, accordingly, values above 100 cm^2 were removed for subsequent analysis

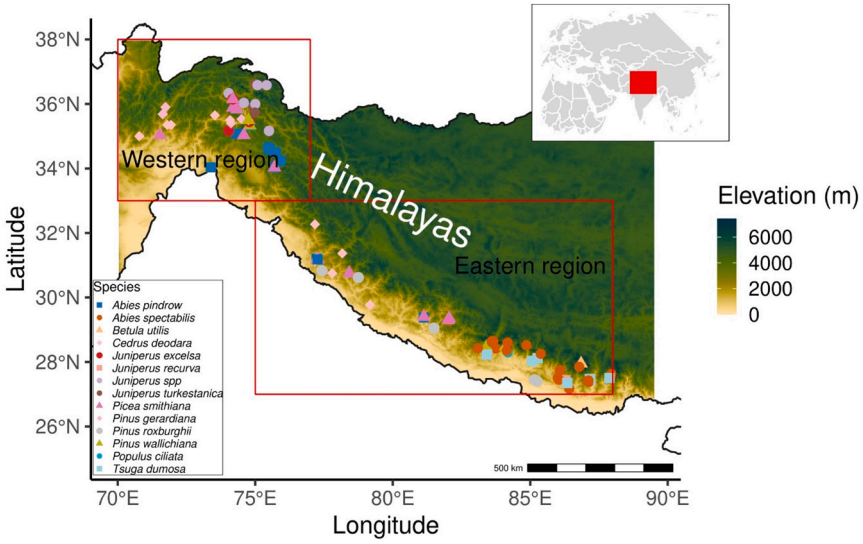

Fig. 1. Location of the study sites showing the sub-regional division into the Western region and Eastern region. Longitude and latitude are represented in the x- and y-axis, respectively. Hindu Kush Himalayan region (HKH) boundary is depicted by black line, while elevation gradients are showed by green color gradient. The included tree species and sampling locations are depicted as symbols.

(accounting for <0.003 % of the total samples).

2.2. Climate data

Long-term climate records from the HKH region are scarce and meteorological stations are often far away from the sampling sites. To obtain a reliable climate dataset, comparable among sampling sites, we obtained total monthly precipitation and mean monthly temperature data from the Climate Research Unit TS4.05 global climate database (*CRU:* Harris et al., 2020; *Climate Explorer*, 2021). We downloaded these climate values from the years 1901 to 2020 with a cell resolution of *0.5°* × *0.5°*, which resulted in a total of 39 unique climate cells for our study area. We computed seasonal total (sum) precipitation and mean (average) temperature for winter (December of the prior year, January and February of the current year; Pwi, Twi, respectively); spring (March, April and May of the current year; Psp, Tsp, respectively); summer (June, July and August of the current year; Psu, Tsu, respectively); autumn (September, October and November of the current year; Pau, Tau, respectively). In addition, we included summer and autumn of the previous year (Paup, Taup, respectively) as climatic conditions of the previous year may significantly modulate growth (Fritts, 1976).

Future climate data were obtained from mean monthly temperature and total monthly precipitation estimates available for two study cells: Eastern region (27.5–30°N, 80–82.5°E) and Western region (35–37.5°N, 72.5–75°E). These data were obtained at the highest possible resolution (*2.5°* × *2.5°*) using multi-model means from 32 General Circulation Models of the Climate Model Intercomparison Project (CMIP5) for the Representative Concentration Pathways (RCPs) 2.6, 4.5, 6.0, and 8.5. Climate data were averaged according to the seasons explained above (Supplementary material Table S1).

2.3. Linear mixed effect models

We applied Linear Mixed-Effects Models (LMMs) using the age-effect residuals as the response variable. Seasonal climate variables (e.g., temperature and precipitation for spring, summer, and annual periods) were included as fixed effects. Each individual tree's BAI was included as a random factor to account for repeated measures and individual variability. Site elevation was tested as a covariate. For the first step, age-effect models were performed for each species and region by testing polynomial and sigmoidal regressions. The residuals from these age-effect models, which represent growth variability not explained by age, were used in the subsequent climate sensitivity analyses. Stepwise variables selection was performed starting from a saturated model that includes all the seasonal climate variables for both temperature and precipitation. Then, iterations were performed after removing the less significant variables, based on the Akaike Information Criterion (AIC). the most reliable model was the one with the lowest AIC value in case of models with <2 units of difference in their AIC values, the model with less fixed factors was chosen based on parsimony principle (a simpler model with fewer parameters is favored over more complex models with more parameters, provided the models fit the data similarly well) (Jiang and Nguyen, 2007; Cavanaugh and Neath, 2019). Finally, the residuals were obtained and tested for first-order autocorrelation by using the previous year BAI as predictor. BAI prediction was then obtained as the sum of the age, climate, and autocorrelation estimates (Matías et al., 2017). The packages "nlme" and "mgcv" were used in the IDE RStudio of the R programming language (*R: The R Project for Statistical Computing*, 2021; *RStudio | Open source & professional software for data science teams*, s. f., n.d.). The structure of the model is as follows:

$$BAI_{ijt\sim}\beta_0 + \sum_{k=1}^{n} \beta_k \cdot C_{jt}^{(k)} + \beta_2 \cdot E_j + u_i + \varepsilon_{ijt} \quad \text{(ii)}$$

where: BAI_{ijt} = BAI Residual of the tree i at site j in year t

$C_{jt}^{(k)}$ = Seasonal climate variable k (e.g., temperature or precipitation in spring, summer, autumn and Winter), E_j = Elevation of site j (covariate), $\beta_k, \beta_0, \beta_2$ = Fixed effect coefficients, u_i = Random intercept and ε_{ijt} = Residual error.

2.4. Growth predictions and validation

Growth forecast for each tree species and region (Eastern and Western), were performed by running the obtained models under different climate scenarios (climate model predictions) between 1950 and 2100 using the final growth model (Taylor et al., 2012) in Equation (ii). Finally, predictions were obtained based on the growth model, by simulating 1000 trees with ages randomly generated between 3 and 100 year as starting point (Matías et al., 2017). The dataset comprising observed and predicted BAI was partitioned into training and testing subsets to evaluate the predictive accuracy of the LMMs. Datasets of each species containing individual trees from different sites were randomly assigned to the training set with 80 % of the data which was used to develop the models, while the remaining 20 % was reserved as the testing set for validation purposes (Raschka, 2020). This approach ensured that the models were evaluated on unseen data providing an unbiased measure of their performance. Model performance, comparing observed BAI with predicted values, was assessed using the following metrics: Coefficient of Determination R^2, Root Mean Squared Error (RMSE), Mean Absolute Error (MAE) and Nash-Sutcliffe Efficiency (NSE) (Krause et al., 2005; Legates and McCabe, 1999; Nash and Sutcliffe, 1970; Willmott and Matsuura, 2005). Metrics were calculated for both training and testing datasets to evaluate the model fit, accuracy and generalization. A value of NSE > 0 indicates satisfactory model performance (Nash and Sutcliffe, 1970).

3. Results

3.1. Current and future climate trends

Climate data showed contrasting precipitation and temperature patterns for all the seasons in both, the Eastern and the Western study regions (Supplementary material, Fig. S1). The Eastern region is relatively moist and warm, while the Western region is relatively dry and cold (Table 1). On average, the Eastern region recorded a mean total annual precipitation of roughly 1300 mm, while the Western region received on average about 400 mm of total annual rainfall (Table 1). Nonetheless, the mean variability in precipitation is relatively high in both regions. Mean annual temperatures also showed differences between the two regions. The Eastern region is warmer with a mean temperature of 9.6 °C, while the Western region reported mean values of 2.9 °C. The difference between maximum and minimum temperatures was greater in the Eastern region (24.2 °C and −7.6 °C, respectively) compared to the Western region (18.3 °C and −5.0 °C, respectively) (Table 1).

Seasonal climate analysis indicated significant differences ($p < 0.05$) in mean temperature and precipitation between the two regions. During winter, the Western region was colder, with average temperatures of −7.9 °C and wetter (108.1 mm). In contrast, the Eastern region reported warmer temperatures of 1.7 °C and lower precipitation of (74.7 mm). In spring, the Western region continued to have lower temperatures, averaging 2.0 °C with precipitation of about 143.1 mm. Eastern region was warmer in spring, with average temperatures of 10.0 °C, and wetter with 187.4 mm/year of precipitation. During summer, the Eastern region was warmer, with average temperatures of 16.0 °C and significantly higher precipitation of 786.2 mm. The Western region showed average summer temperatures of 12.3 °C and 114.1 mm of precipitation. Finally, in autumn, temperatures in the Eastern region were higher, averaging 10.2 °C with 244.4 mm of precipitation, whereas the Western region exhibited cooler temperatures, averaging 4.0 °C and 56.5 mm of precipitation, respectively (Table 1).

Table 1
Seasonal total (sum) precipitation (mm) and mean (average) temperature (°C) for winter (December of the prior year, January and February of the current year; Pwi, Twi, respectively); spring (March, April and May of the current year; Psp, Tsp, respectively); summer (June, July and August of the current year; Psu, Tsu, respectively); autumn (September, October and November of the current year; Pau, Tau, respectively); annual mean temperature (Ty) and total precipitation (Py). Eastern (top) and Western (bottom) regions for the period 1901–2020.

Region	Statistics	Twi	Tsp	Tsu	Tau	Pwi	Psp	Psu	Pau	T_Y	P_Y
Eastern	Mean	1.7	10	16	10.2	74.7	187.4	786.2	244.4	9.6	1293
	Max	17.3	26.4	28.8	25.2	341.1	549.8	2290	836.2	24.2	4017
	Min	−16.1	−9.5	0.4	−7.5	0.7	11.2	24.4	9.4	−7.6	46
	St. dev.	8	8.3	6.4	7.6	45.1	92.5	405	147.6	7.6	651
Western	Mean	−7.9	2	12.3	4	108.1	143.1	114.1	56.5	2.9	422
	Max	9.7	19.9	26.1	19.5	410.1	507.4	1122	494.5	18.3	2534
	Min	−19.3	−7.6	5	−4.3	10.5	14.7	2	2.6	−5	30
	St. dev.	4.8	4.6	3.9	4.2	55	68.1	114.4	40.3	4.3	409

Abbreviations: Maximum (Max), Minimum (Min), and Standard Deviation (St. Dev.)

Analysis of CMIP5 climate data for the different scenarios showed a projected increase both in temperature and precipitation in both regions throughout the 21th century (Supplementary material, Table S1; Figs. S2–S3). Temperature rise is expected to occur in all seasons, except for RCP 2.6, which predicted steady temperature trends. Precipitation, instead, is expected to decrease during winter and spring in the Eastern region (Supplementary material, Fig. S2). However, an overall increasing trend was observed in the Western region precipitation forecasting (Supplementary material, Fig. S3). The temperature rise is forecasted to be lower in the Eastern region than the Western region (ANOVA, $p < 0.05$; Supplementary Table S3, Figs. S2–S3).

3.2. Tree growth rates

The analysis of growth trends showed significantly lower mean BAI for the Western region (6.67 cm^2/year) than the Eastern region (9.89 cm^2/year). The maximum and minimum BAI values were also significantly different between zones. In the Western region, the minimum mean BAI was 0.82 cm^2/year for the population of *Juniperus* spp., growing at 3600 m elevation, while the maximum mean BAI was 18.09 cm^2/year for the population of *Picea smithiana*, growing at 2900 m elevation. In the Eastern region, the minimum mean BAI was 1.48 cm^2/year for the population of *Betula utilis*, growing at 4100 m elevation, while the maximum was mean BAI 23.96 cm^2/year for the population of *Pinus roxburghii*, growing at 1750 m elevation.

3.3. Tree species sensitivity to climate

After performing the lLMMs, we found that the models which included the effect of elevation had lower AIC than those which did not consider it, except for *Abies pindrow* and *Pinus wallichiana* and *Juniperus excelsa* in which a slight decrease of around 2 points of AIC was obtained including elevation in the model. Overall, models including elevation maintained the sensitivity to the same climatic variables, with the exception of *Picea smithiana*, *Tsuga dumosa* and *Abies pindrow*.

Regarding the climatic sensitivity of the different species, we observed that *Picea smithiana* and *Pinus roxburghii* exhibited positive responses to winter and autumn temperatures (Twi and Tau) as well as to precipitation (Pau, Pwi and Psp) (Table 2). On the contrary, all except *Pinus roxburghii*, showed a negative response to spring and summer temperatures (Tsp and Tsu). In the Eastern region, most of the species showed negative responses to summer temperatures and positive responses to winter temperatures. The only species, located at the highest elevation, *Betula utilis*, showed positive sensitivity to spring temperature (Table 2). In general, temperature (positive or negative) was the dominant driver of tree growth in the Eastern region.

In the Western region, we recorded that growth of all *Juniperus* species (*J. excelsa*, *J.* sp., *J. turkestanica*, *J. komarovii*) showed negative correlation with summer temperature (Table 2). for the rest of the species, temperature generally had positive influence except for winter and spring temperatures in *Pinus wallichiana* and spring temperatures in *Picea smithiana*. The effect of precipitation was positive in all the seasons, except for autumn in *Juniperus excelsa* for which the effect was negative (Table 2). Overall, temperature remained the main driver of growth.

3.4. Fitting and model validation

Growth models showed overall reliable fits for all the studied tree species (Supplementary Material, Fig. S4). Nonetheless, we obtained contrasting patterns among the relative weights of age effects, climate sensitivity and autocorrelation models. In the Eastern region, age-effects explained on average about 5 % of the total growth variance, while it ranged from practically zero effect modeling the growth of *A. pindrow*, to significant contributions in the growth pattern of *B. utilis*, explaining 13 % of the observed growth variance (Table S2, Fig. 2a). In the Western region, age-effect models contributed slightly less variance (3–10 %) (Table S2 and Fig. 2b).

Climate variables explained a greater portion of growth variance in the Western region (60 %) compared to the Eastern region (48 %). *Juniperus turkestanica* showed the highest climate variance (76 %) in the Western region, while *Abies spectabilis* was highest in the Eastern region (55 %). Autocorrelation accounted for a similar share of variance in both regions, with slightly higher values in the Eastern (average 21 %) compared to the Western region (20 %). The highest autocorrelation effect was seen in *Tsuga dumosa* (28 %) and *Juniperus excelsa* (29 %) for the Eastern and Western region, respectively (Fig. 2a and b).Overall, most of the species exhibit robust model performance with consistently high R^2, low RMSE and MAE, and strong NSE values (>0.50) across both training and test datasets, while the species *Tsuga dumosa* and *Populus ciliata* demonstrate poor performance indicated by low R^2, high error metrics, and negative or very low NSE in the test data (Fig. S4). For *Populus ciliata*, the poor test performance might relate to very low sample size (n = 3 sites) used for the test data, while for *Tsuga dumosa*, the large standard deviation difference in both BAI and predicted BAI indicates that the tree population in the test data contains values outside the training data.

3.5. Projected tree growth under future climate

The two regions differed in the forecasting BAI for the 21st century (Fig. 3a & b). The Eastern region yielded strong negative BAI trends for *P. roxburghii* (55–67 %) that even exhibit no growth at the end of the series under all RCP scenarios (Fig. 3a). The projected BAI for *Cedrus deodara* shows divergent regional trends: in the Eastern region, all scenarios projected BAI decline of 23–40 %, while the Western region shows a moderate growth improvement of 7–15 %. Likewise, *Pinus wallichiana* shows a slight decrease in the Eastern region by 7.6–9.4 % across scenarios but improved growth in the Western region. *Abies pindrow* nearly doubles its BAI in the Eastern region across all scenarios

Table 2
Climate sensitivity obtained for each species separated by region (Eastern and Western). Selected climate variables are noted in blue/orange font indicating significant positive/negative correlation, respectively. Mean elevation of the sampling locations is also shown.

Region	Species	Climate sensitivity (selected variables)	Elevation
Eastern	*Betula utilis*	Tsp	4100
	Abies spectabilis	Twi+Tsp+Tsu+Tau+Pwi+Psp+Psu	3250
	Pinus wallichiana	Tau+Pau+Pwi	3050
	Abies pindrow	Tau+Tsu+Pwi+Psp+Psu	3000
	Picea smithiana	Twi+Tsp+Tsu+Tau+Psp	2850
	Tsuga dumosa	Twi+Tsu+Tau+Psp+Psu+Pau	2800
	Cedrus deodara	Twi+Tsp+Tsu+Tau+Pwi+Psp	2400
	Populus ciliata	Tau+Tsp+Psp	2270
	Pinus roxburghii	Twi+Tsp+Tsu+Tau+Pwi+Psp+Psu	1750
Western	*Juniperus turkestanica*	Tsp+Pwi+Psp	3750
	Juniperus recurva	Twi+Tsu+Psu	3550
	Juniperus spp	Twi+Tsu+Pwi+Psp	3480
	Picea smithiana	Tau+Twi+Tsp+Tau+Pau+Pwi+Psp	3200
	Pinus wallichiana	Tau+Twi+Tsp+Tsu+Pwi	3150
	Juniperus excelsa	Taup+Twi+Tsp+Tsu+Tau+Pwi+Psp+Psu+Pau	3140
	Abies pindrow	Taup+Tsu+Tau+Psu	3000
	Cedrus deodara	Twi+Tsp+Tsu+Tau+Pwi+Psp+Pau	2720
	Pinus gerardiana	Twi+Tsu+Paup+Pwi+Psp+Psu	2250

(95–108 %) and shows a pronounced 299 % BAI increase in the Western region. Broadleaved tree *Betula utilis* maintain relatively low growth rates overall, because it may benefit only modestly from future climate conditions with the most favorable outcomes under RCP 2.6. In contrast, other species showed increases in BAI in this zone, with *J. recurva* showing the greatest BAI increases. *Abies spectabilis* in the Eastern region revealed only slight improvements (5–7 %) in BAI under future climate conditions. Within the Western region, only two species (*Juniperus* spp.) and *Pinus gerardiana* are projected to undergo declining BAI under moderate to high emission scenarios (RCP 4.5–8.6), however, moderate improvement expected in both the species under RCP 2.6 scenario. Other juniper species (*Juniperus turkestanica Komar* and *Juniperus excelsa M.-Bieb*) in the Western region showed consistent gain in BAI under all the climate scenarios (Fig. 3b). Overall, the Eastern region experiences growth declines (7–67 %) for *Pinus roxburghii*, *Cedrus deodara*, and *Pinus wallichiana* across all RCPs, while *Abies pindrow* shows growth enhancement (95–108 %) under all scenarios. In contrast, the Western region generally exhibits widespread increases (5–299 %) across most species under all RCPs, except for *Juniperus* spp. and *Pinus gerardiana*, which decline (5–15 %) under moderate to high emissions (RCP 4.5–8.5) but exhibit moderate gains (5–10 %) under RCP 2.6.

4. Discussion

4.1. Species specific growth patterns in relation to climate

The present study shows that the influence of temperature on tree growth is generally stronger (both negatively and positively) than of precipitation. In *B. utilis*, for instance, no significant effect of rainfall was found for any season of the year. This observation is in agreement with several other studies where temperature was also found the main environmental factor driving tree growth at high altitudes and latitudes (Camarero et al., 2015; Dhyani et al., 2021; Rossi et al., 2008; Shi et al., 2021a, 2021b; St. George, 2014).

We observed that winter temperatures had a positive effect, on tree growth in the Eastern region. This region experiences a monsoonal climate with abundant rainfall (Bhattacharyya et al., 2023). Warmer winter temperature promotes root activity (Dhyani et al., 2021; Qi et al., 2015), decreases the number of frost days (Fan et al., 2009; Körner, 1998) and frost severity resulting in enhanced water availability (Ning et al., 2012; Shi et al., 2021b) for photosynthesis and the evaporative demand. All tree species, except *A. pindrow* in the Eastern region showed positive correlations with winter precipitation. (Bhattacharyya et al., 2023; Zhang et al., 2018). This condition is relevant in high-elevation areas where persistent snow cover may delay the onset of cambial activity, thereby shortening the growing season and negatively impacting growth. Other species may benefit from winter temperatures that remain just above critical limits allowing physiological processes to continue (Zheng et al., 2022). Across both regions, trees exhibited a negative growth response to spring temperatures due to increased evapotranspiration and moisture deficits during a period of rapid physiological demand (Bhattacharyya et al., 2023). Conversely, spring precipitation was positively correlated with growth indicating that sufficient moisture availability during this period plays a critical role in supporting early-season physiological processes and mitigating temperature-induced water stress (Singh and Yadav, 2005). This negative effect of spring warming was evident even at higher elevations suggesting that warming may exceed species-specific thermal optima or exacerbate moisture limitations if not accompanied by sufficient precipitation (Bhattacharyya and Yadav, 1999; Dhyani et al., 2022a, 2022b; Shi et al., 2021a, 2021b; Bhattacharyya et al., 1988; Liang et al., 2014).

We observed that most of the species showed a negative response to high summer temperatures in both, Eastern and Western regions. Both zones encounter elevated temperatures in the summer season, which leads to increased evapotranspiration, moisture deficits and reduced tree growth (Bhattacharyya et al., 2023). This observation is contradictory to several other studies from the high mountainous region (Deslauriers et al., 2003; Liang et al., 2016; Matías et al., 2017; Mu et al., 2021; Rossi et al., 2008; Shi et al., 2021a, 2021b; George, 2014). The response to summer temperature in both regions depends on availability of summer rainfall. In the Western region, summer rainfall is low or highly variable and even in the Eastern monsoonal region rainfall can be erratic or delayed which makes trees vulnerable to mid-season drought stress (Zheng et al., 2021). As a result, elevated summer temperatures when not matched by adequate and well-timed rainfall can significantly limit growth in sites with shallow soils or poor water holding capacity. In the Western region, tree growth demonstrated a predominantly positive correlation with precipitation during the summer monsoon period, while in the moist Eastern region, it exhibited a negative correlation. Therefore, it is anticipated that an increase in summer rainfall will likely enhance the growth rate in the dry zone (Candel-Pérez et al., 2012; Dhyani et al., 2022a, 2022b; Herrero et al., 2013; Matías et al., 2017; Sánchez-Salguero et al., 2015), while in the Eastern region where there was no water limitation, the increased rainfall along with increased cloudiness is likely to adversely affect tree growth (Zhang et al., 2018).

4.2. Tree growth responses to future warming

The spatial variability in growth among species revealed a distinct West–East responses to future warming closely aligned with regional differences in seasonal precipitation variability and moisture availability. Considering the situation of increasing temperatures and without change in precipitation, we found that species located in the Eastern region could be adversely affected by water stress. This stress could severely impact species like *Cedrus deodara* and *Pinus roxburghii*, which are projected to experience substantial declines in BAI, in some cases, with little or no growth by the end of the century. Under extreme water stress tree mortality may be common (Bhattacharyya et al., 2023; Klesse et al., 2020, 2024; Martinez del Castillo et al., 2022; Matskovsky et al., 2021; Sánchez-Salguero et al., 2017a, 2017b).

Despite these challenges, certain species in the Eastern region are expected to maintain or even improve growth under future climate scenarios. Species *A. pindrow* and *J. recurva* in the Eastern region, likely to show increased growth in this region under moderate to severe (RCP 4.5–8.5) climate change conditions Both species responded positively to rising summer temperatures which plays a crucial role in their seasonal growth development. For *A. pindrow*, xylogenesis occurs from April to September, with peak tracheid formation in summer indicating the role

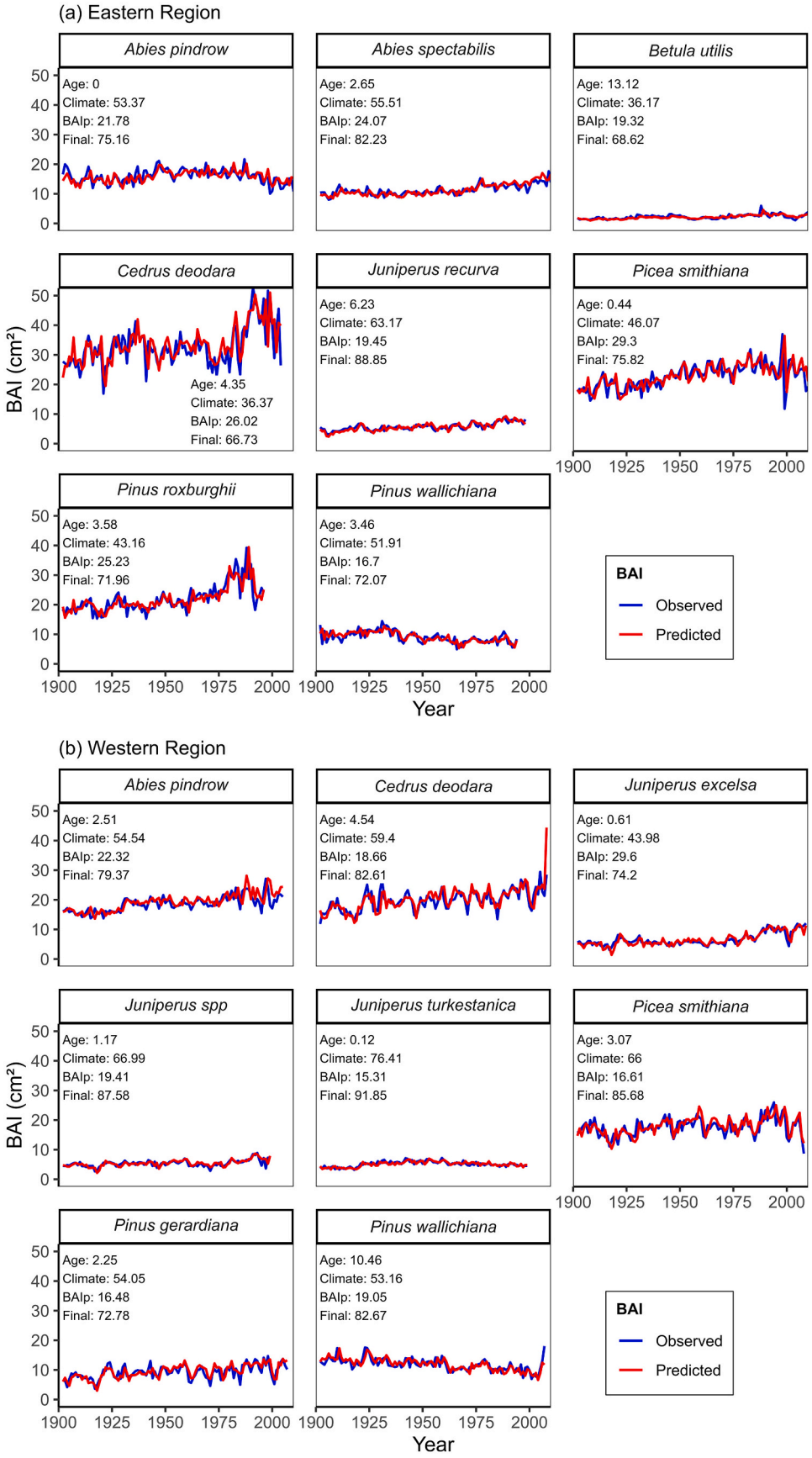

Fig. 2. Observed (blue line) and predicted (red line) basal area increment (BAI, cm^2) for each species studied in the Eastern (a) and Western region (b). The insets indicate the relative weights of each growth component (age-effect, climate sensitivity, autocorrelation BAI) and the final fit of the LMMs, expressed as the percentage of explained variance.

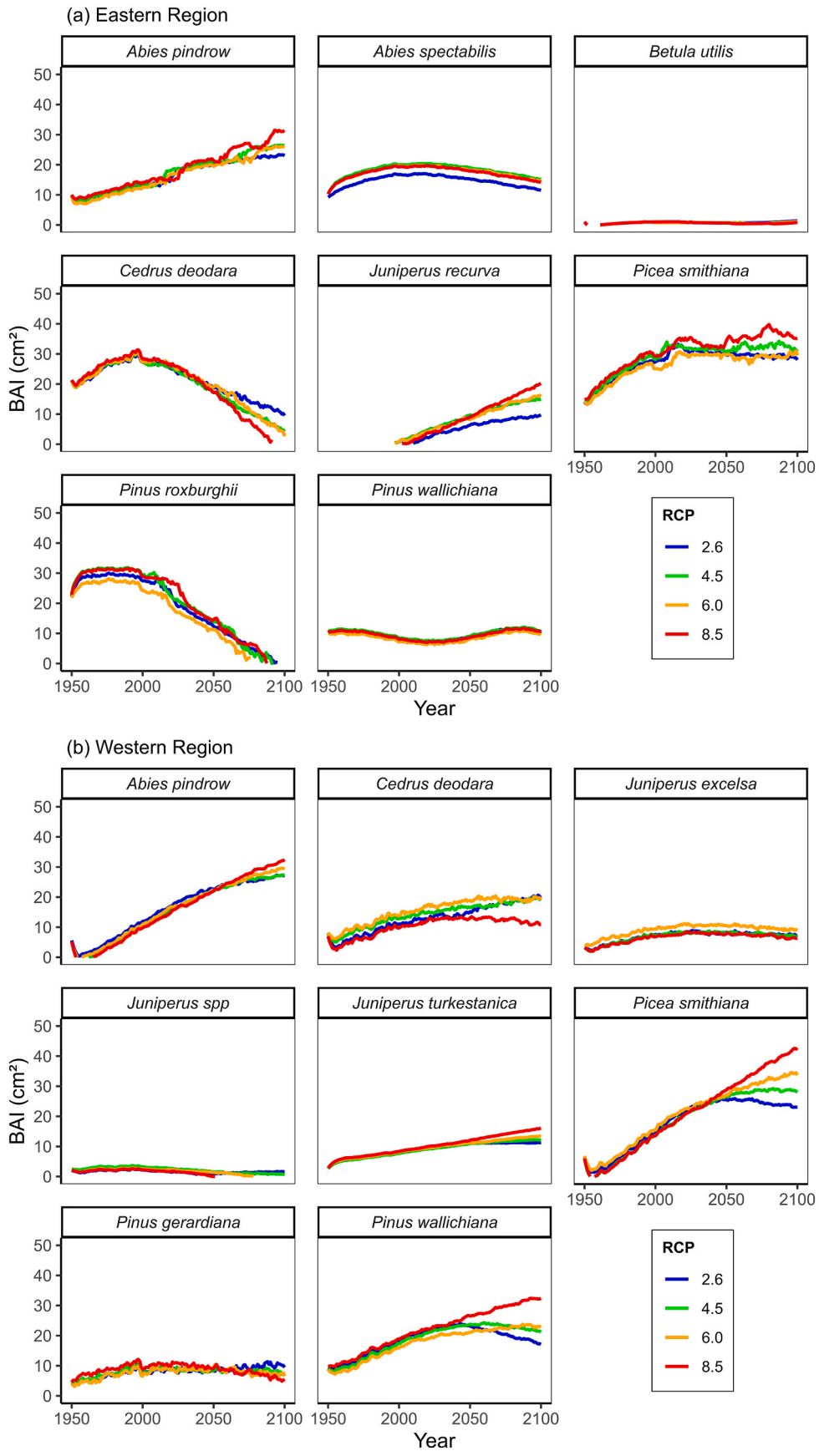

Fig. 3. Basal area increment (BAI, cm^2) forecasting obtained under different RCP scenarios (*RCP2.6*; *blue*, *RCP4.5*; *green*, *RCP6.0*; *orange*, *RCP8.5*; *red*) for Eastern (a) and Western (b) region.

of warm temperatures in extending the growing season and enhancing radial growth at higher altitudes (Malik et al., 2020). Likewise, warm summers are responsible for higher growth rates in *J. recurva* and a greater root development favoring a greater accumulation of carbohydrates that allows a higher wood production during the growing season (Fan et al., 2010; Gou et al., 2008).

In the Western region, *A* larger number of conifer species is projected to thrive under future climate conditions. *A. pindrow*, *Picea smithiana*, *J. turkestanica* and *Pinus wallichiana* are all predicted to maintain higher growth rates by the end of 21st century even under most extreme climate scenario RCP 8.5. This enhanced growth is likely associated with the projected increase in frequency of Western disturbances and a higher likelihood of snowfall in the Western Himalaya and Karakoram region (Krishnan et al., 2019). Improved future precipitation in the Western region would synchronize tree growth with snowmelt water which provides essential soil moisture to rehydrate tissues, initiate cambial growth, support photosynthesis and sustain early season growth (Bhattacharyya et al., 2023).

Some species-level responses also reflected seasonal climatic sensitivities in the Western region. We observed that limitation of growth in *A. pindrow* was found due to cold temperatures in the growing seasons which implies that any increase in temperatures during this period is associated with an increase in growth rates (Malik et al., 2020). However, the observed positive response of this species to autumn temperature may be related to the presence of a thin snow cover which prevents water deficits at the end of the growing season and thus the predicted increase in autumn temperature could contribute to growth stabilization of this species in the 21st century.

For *P. smithiana*, we observed that the increase in temperature in most of the seasons except spring, favored growth. Notably, in this species the positive effect of increasing temperature continued up to the highest temperature scenario. *J. turkestanica* showed positive correlations with spring temperatures together with spring rainfall, which reinforces the conclusions of other studies that wet springs are key for the growth of this species (Opała-Owczarek et al., 2023). This suggests at the locations that we studied growth is limited by low temperatures and low humidity during critical growing periods. Interestingly, *P. wallichiana* presented positive responses to the previous autumn and summer temperatures, with the summer period being the most influential. This contradicts the results obtained for *Juniperus* spp. and *P. gerardiana* which were the only species in the Western region that showed a decrease in growth. This trend is observed for all models, being more accentuated in harsher climatic scenarios. This species appears to be favorable, but overshadowed by the negative effect of increasing summer temperatures. Continued warming may exacerbate water stress in *Juniper* spp. lead to the disappearance of this species in the study region. Past observations already point to its vulnerability; long-term tree-ring records from Juniperus trees in the Himalaya reveal sharp declines in growth during historically warm and dry periods marked by high temperatures and increased aridity (Esper, 2000; Esper et al., 2002). Without sufficient moisture, *Juniperus* spp. may face a significant risk of local disappearance under future climate conditions.

Our study highlights that the species of monsoon dominated areas (Eastern region) and those under the influence of westerlies (Western region) tend to respond differently to climate change in terms of tree growth. However, because of the paucity of data it is difficult to make convincing generalizations. Management practices for tree species of monsoon dominated climate may differ from those occurring in areas under the influence of westerlies. To understand future changes, it is important to undertake long-term studies on species in both regions and with species of various growth forms. For example, drought responses of conifers considerable differ from broadleaved species (Singh and Zobel, 2025). Generally, hydraulic safety margin is wider in conifers than in oaks and other broadleaved species. Such differences in hydraulic strategy indicate that conifers may be more resilient to drought conditions, whereas broadleaved species (e.g. *Betula utils* in the present study) may be more vulnerable to growing season water stress under projected climatic shifts (Pandey et al., 2018). Therefore, management practices should consider these differences with a focus on enhancing drought resistance in broadleaved species through selective soil moisture conservation and targeted reforestation efforts.

Growth improvement and consequent range shift in tree species in the Western region driven by westerlies may reduce grassland areas, requiring frequent grazing to control tree encroachment and preserve grassland ecosystems. In several areas vegetation is close to summits, left with little space to move upward. Many species treelines are adversely affected by warmer condition because of the lack of space to migrate. Transboundary cooperation among the Himalayan countries can go a long way in protecting species by facilitating lateral species movement.

4.3. Limitations and uncertainties

Our LMM rely on climate-growth relationships derived from a calibration period (20th century) and projections based on climate scenarios (21st century). One advantage of using a LMM approach is its ability to perform well with low site replication and to account for unquantified factors, thus producing more robust estimates of climate sensitivities across the distribution of trees (Klesse et al., 2020). However, such modeling operates under the assumption that climate response remains constant over time, which hinders the identification of the adaptive capacity of trees to climate changes. As a result, if the future growth response of some species shows non-linear responses, the resulting growth patterns may differ from our predictions (Matskovsky et al., 2021). With more meta-data it would be possible to make the LMM more realistic by adding the tree- and site-level influences as random effects into the list of fixed effects, such as tree genotype, site characteristics, forest stand conditions, and disturbances that are routinely collected in forest inventories or permanent sample plots (Canham et al., 2018; Klesse et al., 2020; Wilmking et al., 2020). Furthermore, the LMMs do not account for the physiological impact of increased atmospheric CO_2 and potential changes in water use efficiency (WUE) (Andreu-Hayles et al., 2011; Groenendijk et al., 2015; Marchand et al., 2020; Rahman et al., 2020).

Other than linear models, use of process-based tree-ring formation models allow a more physiologically based approach for the study of tree growth response to future climate variability compared to linear models, since they combine mixed non-linear responses to climatic changes considering various growth processes according to the principle of limiting factors (Guiot et al., 2014). For instance, the VS-Lite model has been applied quite extensively in non-linear growth modeling with trees in many forest ecosystems because of its possibility of integrating temperature and precipitation simultaneously as principal climatic factors affecting tree growth (Matskovsky et al., 2021; Sánchez-Salguero et al., 2017a, 2017b; Tolwinski-Ward et al., 2011). However, site-specific performance of VS-Lite may be compromised as the model needs absolute temperature and precipitation data which are rare in the Himalaya. In such complex terrain, an estimate based on elevation and lapse rates might not sufficiently cover small scale climate variability (Breitenmoser et al., 2014).

Future climate projections used in the present study are based on General Circulation Models. To account for uncertainties in the models we rely on multimodal means of individual climate model simulations assuming that they are best suited to describe future climatology (Rahman et al., 2018). However, using a multi-model mean for projecting climate change fails to capture the temperature and precipitation variability associated with internal processes. For example, the differences in BAI projections using observed and model data for some species (*A. pindrow*, *J. recurva*, *P. smithiana* and *P. wallichiana*) during 1950–2000 might be related to bias in model data, particularly, overestimation of droughts and underestimation of year to year variability (Nasrollahi et al., 2015). Although we do not expect a significant impact of extreme events on our LMMs, it should be noted that thresholds of tree

growth might be reached sooner considering that year-to-year variability in these climate parameters will be much stronger (Allen et al., 2015; Sánchez-Salguero et al., 2017a, 2017b). Additionally, model projections assume independence in each model simulation, but in reality, large similarity generally appears because of shared parameterizations, boundary conditions, and structural features (Pathak et al., 2023). The similarity leads to projections dominated by the largest set of similar models and thus the projections might be biased in the direction of the consensus from these similar models and hence result in underestimation for the true range of inter-model uncertainty (Lehner et al., 2020; Pathak et al., 2023). This is particularly true in high mountain regions where the complex topography and different climatic conditions make modeling difficult (Dimri et al., 2018; Latonin et al., 2021; Salunke et al., 2019). Therefore, reduced reliability in these regions might also affects future tree growth projection due to underestimation of inter-model uncertainty.

5. Conclusion

We obtained reliable modeling of the species-specific observed and expected basal area increment over a wide environmental gradient in the Himalayas using tree ring-data. Despite limitations, our results provide valuable information to detect vulnerable species and regions under the expected climate change scenarios. Thus, the improvement of climate data, specifically regarding their spatial resolution and the explicit consideration of local orographic effects, may provide more realistic predictions at local scale. Furthermore, climate-growth relationships might be improved, too, considering saturating or non-linear responses, as well as new methods, such as machine learning approaches for predicting tree growth trends based on basal area increment. Our findings support the hypothesis that increasing temperatures during the growing season are likely to reduce growth in the Eastern region, where high rainfall and warmer conditions may lead to heightened evaporative demand and moisture stress. In contrast, species in the Western region appear more resilient with many showing stable or enhanced growth trends, potentially supported by increases in winter and spring precipitation linked to strengthened westerly systems. Several species (*B. utilis*, *P. gerardiana*, *P. wallichiana*, *A. spectabilis*) are expected to maintain an almost steady growth trend, while others (*C. deodara*, *P. roxburghii*) may show growth decline and further forest dieback in the coming future. On average, the Western region showed few study cases (junipers) of growth decline, prevailing the expectations of positive responses. Forests in the Eastern region may need more protection while species in Western region that are more likely to adapt future climate conditions could be used in reforestation and forest management. This study can be incorporated into the Himalayan national guidelines for species and site-specific sustainable forest management highlighting the need of tree ring-based research in policy and practice under ongoing rapid climate change.

CRediT authorship contribution statement

Rupesh Dhyani: Writing – review & editing, Writing – original draft, Validation, Resources, Investigation, Funding acquisition, Formal analysis. **Pablo Casas-Gómez:** Writing – review & editing, Writing – original draft, Validation, Software, Methodology, Investigation, Formal analysis, Data curation, Conceptualization. **Lea Schneider:** Writing – review & editing, Writing – original draft, Validation, Investigation, Formal analysis, Data curation. **Raúl Sánchez-Salguero:** Writing – review & editing, Writing – original draft, Project administration, Investigation, Funding acquisition. **Shinny Thakur:** Writing – review & editing, Writing – original draft, Investigation, Funding acquisition. **Mayank Shekhar:** Writing – review & editing, Writing – original draft, Investigation, Funding acquisition. **Rajesh Joshi:** Writing – review & editing, Writing – original draft, Investigation, Funding acquisition. **Jagdish Chandra Kuniyal:** Writing – review & editing, Writing – original draft, Investigation, Funding acquisition. **Amalava Bhattacharyya:** Writing – review & editing, Writing – original draft, Investigation, Funding acquisition. **Surendra Pratap Singh:** Writing – review & editing, Writing – original draft, Investigation, Funding acquisition. **Juan Carlos Linares:** Writing – review & editing, Writing – original draft, Validation, Supervision, Methodology, Funding acquisition, Formal analysis, Conceptualization.

Funding

This research was funded by Department of Science and Technology, Government of India, under the project "Forest Resources and Plant Biodiversity", National Mission on Sustaining the Himalayan Ecosystem -Task Force-3 (NMSHE TF- 3), Phase-2; Junta de Andalucía, grant number PAIDI, P18-RT-1170; and by the Spanish Ministry of Science and Innovation, grant numbers TED2021-129770B-C22, and PID2021-123675OB-C44. RD and LS supported by the German Science Foundation (DFG) project "SCHN 1645/1-1". SPS, AB, and MS also acknowledge Project No. NMHS2024-25/SC-XIII/MG/SL-16.

Declaration of competing interest

The authors declare the following financial interests/personal relationships which may be considered as potential competing interests: Rupesh Dhyani reports financial support was provided by Department of Science and Technology, Government of India. Juan Carlos Linares reports financial support was provided by Junta de Andalucía, grant number PAIDI, P18-RT-1170. Juan Carlos Linares reports financial support was provided by Spanish Ministry of Science and Innovation, grant numbers TED2021-129770B-C22, and PID2021-123675OB-C44. If there are other authors, they declare that they have no known competing financial interests or personal relationships that could have appeared to influence the work reported in this paper.

Acknowledgements

Authors RD, RJ and JCK thank the Director of NIHE for providing the necessary infrastructure and resources that facilitated the execution of this research work. MS and AB express gratitude the Director of the BSIP, Lucknow, Uttar Pradesh, India.

Appendix A. Supplementary data

Supplementary data to this article can be found online at https://doi.org/10.1016/j.scitotenv.2025.179700.

Data availability

Data will be made available on request.

References

Allen, C.D., Breshears, D.D., McDowell, N.G., 2015. On underestimation of global vulnerability to tree mortality and forest die-off from hotter drought in the Anthropocene. Ecosphere 6 (8), art129. https://doi.org/10.1890/ES15-00203.1.

Anderson-Teixeira, K.J., Herrmann, V., Rollinson, C.R., Gonzalez, B., Gonzalez-Akre, E. B., Pederson, N., Alexander, M.R., Allen, C.D., Alfaro-Sánchez, R., Awada, T., Baltzer, J.L., Baker, P.J., Birch, J.D., Bunyavejchewin, S., Cherubini, P., Davies, S.J., Dow, C., Helcoski, R., Kašpar, J., Zuidema, P.A., 2022. Joint effects of climate, tree size, and year on annual tree growth derived from tree-ring records of ten globally distributed forests. Glob. Chang. Biol. 28 (1), 245–266. https://doi.org/10.1111/gcb.15934.

Andreu-Hayles, L.A.I.A., Planells, Octavi, Gutierrez, Emilia, Muntan, Elena, Helle, Gerhard, Anchukaitis, Kevin J., Schleser, Gerhard H., 2011. Long tree-ring chronologies reveal 20th century increases in water-use efficiency but no enhancement of tree growth at five Iberian pine forests. Glob. Chang. Biol. 17 (6), 2095–2112.

Bhattacharyya, A., Yadav, R.R., 1999. Climatic reconstructions using tree-ring data from tropical and temperate regions of India-a review. IAWA J. 20 (3), 311–316.

Bhattacharyya, A., LaMarche Jr., V.C., Telewski, F.W., 1988. Dendrochronological Reconnaissance of the Conifers of Northwest India.
Bhattacharyya, A., Dhyani, R., Joshi, R., Shekhar, M., Kuniyal, J.C., Ranhotra, P.S., Singh, S.P., 2023. Is survival of Himalayan Cedar (*Cedrus deodara*) threatened? An evaluation based on predicted scenarios of its growth trend under future climate change. Sci. Total Environ. 882, 163630. https://doi.org/10.1016/j.scitotenv.2023.163630.
Biondi, F., Qeadan, F., 2008. A theory-driven approach to tree-ring standardization: defining the biological trend from expected basal area increment. Tree-Ring Res. 64 (2), 81–96. https://doi.org/10.3959/2008-6.1.
Bosela, M., Rubio-Cuadrado, Á., Marcis, P., Merganičová, K., Fleischer, P., Forrester, D.I., Uhl, E., Avdagić, A., Bellan, M., Bielak, K., Bravo, F., Coll, L., Cseke, K., del Rio, M., Dinca, L., Dobor, L., Drozdowski, S., Giammarchi, F., Gömöryová, E., Tognetti, R., 2023. Empirical and process-based models predict enhanced beech growth in European mountains under climate change scenarios: a multimodel approach. Sci. Total Environ. 888, 164123. https://doi.org/10.1016/j.scitotenv.2023.164123.
Breitenmoser, P., Brönnimann, S., Frank, D., 2014. Forward modelling of tree-ring width and comparison with a global network of tree-ring chronologies. Clim. Past 10 (2), 437–449. https://doi.org/10.5194/cp-10-437-2014.
Camarero, J.J., Gazol, A., Galván, J.D., Sangüesa-Barreda, G., Gutiérrez, E., 2015. Disparate effects of global-change drivers on mountain conifer forests: warming-induced growth enhancement in young trees vs. CO_2 fertilization in old trees from wet sites. Glob. Chang. Biol. 21 (2), 738–749. https://doi.org/10.1111/gcb.12787.
Camarero, J.J., Linares, J.C., García-Cervigón, A.I., Batllori, E., Martínez, I., Gutiérrez, E., 2017. Back to the future: the responses of alpine treelines to climate warming are constrained by the current ecotone structure. Ecosystems 20 (4), 683–700. https://doi.org/10.1007/s10021-016-0046-3.
Candel-Pérez, D., Linares, J.C., Viñegla, B., Lucas-Borja, M.E., 2012. Assessing climate–growth relationships under contrasting stands of co-occurring Iberian pines along an altitudinal gradient. For. Ecol. Manag. 274, 48–57. https://doi.org/10.1016/j.foreco.2012.02.010.
Canham, C.D., Murphy, L., Riemann, R., McCullough, R., Burrill, E., 2018. Local differentiation in tree growth responses to climate. Ecosphere 9 (8), e02368. https://doi.org/10.1002/ecs2.2368.
Cavanaugh, Joseph E., Neath, Andrew A., 2019. The Akaike information criterion: background, derivation, properties, application, interpretation, and refinements. Wiley Interdisciplinary Reviews: Computational Statistics 11 (3), e1460.
Chakraborty, A., Joshi, P.K., Sachdeva, K., 2016. Predicting distribution of major forest tree species to potential impacts of climate change in the central Himalayan region. Ecol. Eng. 97, 593–609.
Cook, E.R., Krusic, P.J., Jones, P.D., 2003. Dendroclimatic signals in long tree-ring chronologies from the Himalayas of Nepal. Int. J. Climatol. 23 (7), 707–732. https://doi.org/10.1002/joc.911.
CRU: Climate Explorer, 2021. https://climexp.knmi.nl/selectfield_obs.cgi?id=someone@somewhere.
Cuo, L., Zhang, Y., Wang, Q., Zhang, L., Zhou, B., Hao, Z., Su, F., 2013. Climate change on the northern Tibetan Plateau during 1957–2009: spatial patterns and possible mechanisms. J. Clim. 26 (1), 85–109. https://doi.org/10.1175/JCLI-D-11-00738.1.
Delzon, S., Loustau, D., 2005. Age-related decline in stand water use: sap flow and transpiration in a pine forest chronosequence. Agric. For. Meteorol. 129 (3–4), 105–119. https://doi.org/10.1016/j.agrformet.2005.01.002.
Deslauriers, A., Morin, H., Begin, Y., 2003. Cellular phenology of annual ring formation of *Abies balsamea* in the Quebec boreal forest (Canada). Can. J. For. Res. 33 (2), 190–200. https://doi.org/10.1139/x02-178.
Dhyani, R., Bhattacharyya, A., Rawal, R.S., 2021. The oldest birch tree in the Western Himalaya depicting signature of major climatic events of the recent era in its tree rings. Curr. Sci. 121 (03), 350–353. https://www.currentscience.ac.in/Volumes/121/03/0350.pdf.
Dhyani, R., Bhattacharyya, A., Singh Rawal, R., Joshi, R., Shekhar, M., Singh Ranhotra, P., 2022a. Is tree ring chronology of blue pine (*Pinus wallichiana* A. B. Jackson) prospective for summer drought reconstruction in the Western Himalaya? J. Asian Earth Sci. 229, 105142. https://doi.org/10.1016/j.jseaes.2022.105142.
Dhyani, R., Joshi, R., Ranhotra, P.S., Shekhar, M., Bhattacharyya, A., 2022b. Age dependent growth response of *Cedrus deodara* TO climate change in temperate zone of Western Himalaya. Trees For. People 8, 100221. https://doi.org/10.1016/j.tfp.2022.100221.
Dhyani, R., Bhattacharyya, A., Joshi, R., Shekhar, M., Kuniyal, J.C., Ranhotra, P.S., 2023. Tree rings of Rhododendron arboreum portray signal of monsoon precipitation in the Himalayan region. Front. For. Glob. Change 5.
Dimri, A.P., Kumar, D., Choudhary, A., Maharana, P., 2018. Future changes over the Himalayas: mean temperature. Glob. Planet. Chang. 162, 235–251. https://doi.org/10.1016/j.gloplacha.2018.01.014.
Esper, Jan, 2000. Long-term tree-ring variations in Juniperus at the upper timber-line in the Karakorum (Pakistan). The Holocene 10 (2), 253–260.
Esper, J., Schweingruber, F.H., Winiger, M., 2002. 1300 years of climatic history for Western Central Asia inferred from tree-rings. The Holocene 12 (3), 267–277.
Fan, Z.-X., Bräuning, A., Yang, B., Cao, K.-F., 2009. Tree ring density-based summer temperature reconstruction for the central Hengduan Mountains in southern China. Glob. Planet. Chang. 65 (1), 1–11. https://doi.org/10.1016/j.gloplacha.2008.10.001.
Fan, Z.-X., Bräuning, A., Tian, Q.-H., Yang, B., Cao, K.-F., 2010. Tree ring recorded may–august temperature variations since A.D. 1585 in the Gaoligong Mountains, southeastern Tibetan plateau. Palaeogeogr. Palaeoclimatol. Palaeoecol. 296 (1), 94–102. https://doi.org/10.1016/j.palaeo.2010.06.017.
Fritts, H., 1976. Tree Rings and Climate. Elsevier, pp. 14–15.
George, Scott St, 2014. An overview of tree-ring width records across the northern hemisphere. Quat. Sci. Rev. 95, 132–150.
Gou, X., Chen, F., Yang, M., Gordon, J., Fang, K., Tian, Q., Zhang, Y., 2008. Asymmetric variability between maximum and minimum temperatures in Northeastern Tibetan Plateau: evidence from tree rings. Sci. China Ser. D Earth Sci. 51 (1), 41–55. https://doi.org/10.1007/s11430-007-0154-1.
Groenendijk, P., van der Sleen, P., Vlam, M., Bunyavejchewin, S., Bongers, F., Zuidema, P.A., 2015. No evidence for consistent long-term growth stimulation of 13 tropical tree species: results from tree-ring analysis. Glob. Chang. Biol. 21 (10), 3762–3776. https://doi.org/10.1111/gcb.12955.
Guiot, J., Boucher, E., Gea-Izquierdo, G., 2014. Process models and model-data fusion in dendroecology. Front. Ecol. Evol. 2. https://doi.org/10.3389/fevo.2014.00052.
Harris, Ian, Osborn, Timothy J., Jones, Phil, Lister, David, 2020. Version 4 of the CRU TS monthly high-resolution gridded multivariate climate dataset. Scientific data 7 (1), 109.
Herrero, A., Rigling, A., Zamora, R., 2013. Varying climate sensitivity at the dry distribution edge of *Pinus sylvestris* and *P. nigra*. For. Ecol. Manag. 308, 50–61. https://doi.org/10.1016/j.foreco.2013.07.034.
Jiang, J., Nguyen, T., 2007. Linear and Generalized Linear Mixed Models and Their Applications, vol. 1. Springer. https://link.springer.com/content/pdf/10.1007/978-1-0716-1282-8.pdf.
Klesse, S., DeRose, R.J., Babst, F., Black, B.A., Anderegg, L.D.L., Axelson, J., Ettinger, A., Griesbauer, H., Guiterman, C.H., Harley, G., Harvey, J.E., Lo, Y.-H., Lynch, A.M., O'Connor, C., Restaino, C., Sauchyn, D., Shaw, J.D., Smith, D.J., Wood, L., Evans, M. E.K., 2020. Continental-scale tree-ring-based projection of Douglas-fir growth: testing the limits of space-for-time substitution. Glob. Chang. Biol. 26 (9), 5146–5163. https://doi.org/10.1111/gcb.15170.
Klesse, S., Peters, R.L., Alfaro-Sánchez, R., Badeau, V., Baittinger, C., Battipaglia, G., Bert, D., Biondi, F., Bosela, M., Budeanu, M., Čada, V., Camarero, J.J., Cavin, L., Claessens, H., Cretan, A.-M., Čufar, K., de Luis, M., Dorado-Liñán, I., Dulamsuren, C., Buras, A., 2024. No future growth enhancement expected at the northern edge for European beech due to continued water limitation. Glob. Chang. Biol. 30 (10), e17546. https://doi.org/10.1111/gcb.17546.
Knapp, P., Soulé, P., 2011. Increasing water-use efficiency and age-specific growth responses of old-growth ponderosa pine trees in the northern Rockies. Glob. Chang. Biol. 17, 631–641.
Körner, C., 1998. A re-assessment of high elevation treeline positions and their explanation. Oecologia 115 (4), 445–459. https://doi.org/10.1007/s004420050540.
Krause, P., Boyle, D.P., Bäse, F., 2005. Comparison of different efficiency criteria for hydrological model assessment. Adv. Geosci. 5, 89–97. https://doi.org/10.5194/adgeo-5-89-2005.
Krishnan, R., Shrestha, A.B., Ren, G., Rajbhandari, R., Saeed, S., Sanjay, J., Syed, Md.A., Vellore, R., Xu, Y., You, Q., Ren, Y., 2019. Unravelling climate change in the Hindu Kush Himalaya: rapid warming in the mountains and increasing extremes. In: Wester, P., Mishra, A., Mukherji, A., Shrestha, A.B. (Eds.), The Hindu Kush Himalaya Assessment: Mountains, Climate Change, Sustainability and People. Springer International Publishing, pp. 57–97. https://doi.org/10.1007/978-3-319-92288-1_3.
Kumar, S., Khanduri, V.P., 2024. Impact of climate change on the Himalayan alpine treeline vegetation. Heliyon 10 (23), e40797. https://doi.org/10.1016/j.heliyon.2024.e40797.
Latonin, M.M., Bashmachnikov, I.L., Bobylev, L.P., Davy, R., 2021. Multi-model ensemble mean of global climate models fails to reproduce early twentieth century Arctic warming. Polar Sci. 30, 100677. https://doi.org/10.1016/j.polar.2021.100677.
Legates, D.R., McCabe Jr., G.J., 1999. Evaluating the use of "goodness-of-fit" measures in hydrologic and hydroclimatic model validation. Water Resour. Res. 35 (1), 233–241. https://doi.org/10.1029/1998WR900018.
Lehner, F., Deser, C., Maher, N., Marotzke, J., Fischer, E.M., Brunner, L., Knutti, R., Hawkins, E., 2020. Partitioning climate projection uncertainty with multiple large ensembles and CMIP5/6. Earth Syst. Dynam. 11 (2), 491–508. https://doi.org/10.5194/esd-11-491-2020.
Li, X., Liang, E., Gricar, J., Prislan, P., Rossi, S., Cufar, K., 2013. Age dependence of xylogenesis and its climatic sensitivity in Smith fir on the south-eastern Tibetan Plateau. Tree Physiol. 33 (1), 48–56. https://doi.org/10.1093/treephys/tps113.
Liang, E., Dawadi, B., Pederson, N., Eckstein, D., 2014. Is the growth of birch at the upper timberline in the Himalayas limited by moisture or by temperature? Ecology 95 (9), 2453–2465. https://doi.org/10.1890/13-1904.1.
Liang, E., Wang, Y., Piao, S., Lu, X., Camarero, J.J., Zhu, H., Zhu, L., Ellison, A.M., Ciais, P., Peñuelas, J., 2016. Species interactions slow warming-induced upward shifts of treelines on the Tibetan Plateau. Proc. Natl. Acad. Sci. 113 (16), 4380–4385. https://doi.org/10.1073/pnas.1520582113.
Liu, Y., Hoskins, B., Blackburn, M., 2007. Impact of Tibetan orography and heating on the summer flow over Asia. J. Meteorol. Soc. Jpn. Ser. II 85B, 1–19. https://doi.org/10.2151/jmsj.85B.1.
Magnani, F., Mencuccini, M., Grace, J., 2000. Age-related decline in stand productivity: the role ofstructural acclimation under hydraulic constraints. Plant Cell Environ. 23, 251–263.
Mainali, K., Shrestha, B.B., Sharma, R.K., Adhikari, A., Gurarie, E., Singer, M., Parmesan, C., 2020. Contrasting responses to climate change at Himalayan treelines revealed by population demographics of two dominant species. Ecol. Evol. 10 (3), 1209–1222. https://doi.org/10.1002/ece3.5968.
Malik, R., Rossi, S., Sukumar, R., 2020. Variations in the timing of different phenological stages of cambial activity in Abies pindrow (Royle) along an elevation gradient in the north-western Himalaya. Dendrochronologia 59, 125660.
Malik, R.A., Reshi, Z.A., Rafiq, I., Singh, S.P., 2022. Decline in the suitable habitat of dominant Abies species in response to climate change in the Hindu Kush Himalayan

region: insights from species distribution modelling. Environ. Monit. Assess. 194 (9), 596. https://doi.org/10.1007/s10661-022-10245-y.
Manabe, S., Broccoli, A.J., 1990. Mountains and arid climates of middle latitudes. Science 247 (4939), 192–195. https://doi.org/10.1126/science.247.4939.192.
Marchand, W., Girardin, M.P., Hartmann, H., Depardieu, C., Isabel, N., Gauthier, S., Boucher, É., Bergeron, Y., 2020. Strong overestimation of water-use efficiency responses to rising CO_2 in tree-ring studies. Glob. Chang. Biol. 26 (8), 4538–4558. https://doi.org/10.1111/gcb.15166.
Martinez del Castillo, E., Zang, C.S., Buras, A., Hacket-Pain, A., Esper, J., Serrano-Notivoli, R., Hartl, C., Weigel, R., Klesse, S., Resco de Dios, V., Scharnweber, T., Dorado-Liñán, I., van der Maaten-Theunissen, M., van der Maaten, E., Jump, A., Mikac, S., Banzragch, B.-E., Beck, W., Cavin, L., de Luis, M., 2022. Climate-change-driven growth decline of European beech forests. Commun. Biol. 5 (1), 1–9. https://doi.org/10.1038/s42003-022-03107-3.
Matías, L., Linares, J.C., Sánchez-Miranda, Á., Jump, A.S., 2017. Contrasting growth forecasts across the geographical range of Scots pine due to altitudinal and latitudinal differences in climatic sensitivity. Glob. Chang. Biol. 23 (10), 4106–4116. https://doi.org/10.1111/gcb.13627.
Matskovsky, V., Venegas-González, A., Garreaud, R., Roig, F.A., Gutiérrez, A.G., Muñoz, A.A., Le Quesne, C., Klock, K., Canales, C., 2021. Tree growth decline as a response to projected climate change in the 21st century in Mediterranean mountain forests of Chile. Glob. Planet. Chang. 198, 103406. https://doi.org/10.1016/j.gloplacha.2020.103406.
McDowell, N.G., Bond, B.J., Dickman, L.T., Ryan, M.G., Whitehead, D., 2011. Relationships between tree height and carbon isotope discrimination. In: Meinzer, F. C., Lachenbruch, B., Dawson, T.E. (Eds.), Size-and Age-Related Changes in Tree Structure and Function. Springer, Dordrecht, pp. 255–286.
Mu, Y.-M., Zhang, Q.-B., Fang, O., Lyu, L., Cherubini, P., 2021. Pervasive tree-growth reduction in Tibetan juniper forests. For. Ecol. Manag. 480, 118642. https://doi.org/10.1016/j.foreco.2020.118642.
Nash, J.E., Sutcliffe, J.V., 1970. River flow forecasting through conceptual models part I — a discussion of principles. J. Hydrol. 10 (3), 282–290. https://doi.org/10.1016/0022-1694(70)90255-6.
Nasrollahi, N., AghaKouchak, A., Cheng, L., Damberg, L., Phillips, T.J., Miao, C., Hsu, K., Sorooshian, S., 2015. How well do CMIP5 climate simulations replicate historical trends and patterns of meteorological droughts? Water Resour. Res. 51 (4), 2847–2864. https://doi.org/10.1002/2014WR016318.
Ning, B., Yang, X., Chang, L., 2012. Changes of temperature and precipitation extremes in Hengduan Mountains, Qinghai-Tibet Plateau in 1961–2008. Chin. Geogr. Sci. 22 (4), 422–436. https://doi.org/10.1007/s11769-012-0549-6.
Opała-Owczarek, M., Owczarek, P., Rahmonov, O., Małarzewski, Ł., Chen, F., Niedźwiedź, T., 2023. Divergence in responses of juniper tree rings to climate conditions along a high-mountain transect in the semi-arid Fann Mountains, Pamir-Alay, western Tajikistan. Ecol. Indic. 150, 110280. https://doi.org/10.1016/j.ecolind.2023.110280.
Pandey, Sudip, Carrer, Marco, Castagneri, Daniele, Petit, Giai, 2018. Xylem anatomical responses to climate variability in Himalayan birch trees at one of the world's highest forest limit. Perspectives in Plant Ecology, Evolution and Systematics 33, 34–41.
Pathak, R., Dasari, H.P., Ashok, K., Hoteit, I., 2023. Effects of multi-observations uncertainty and models similarity on climate change projections. Npj Clim. Atmos. Sci. 6 (1), 1–12. https://doi.org/10.1038/s41612-023-00473-5.
Qi, Z., Liu, H., Wu, X., Hao, Q., 2015. Climate-driven speedup of alpine treeline forest growth in the Tianshan Mountains, Northwestern China. Glob. Chang. Biol. 21 (2), 816–826. https://doi.org/10.1111/gcb.12703.
R: The R Project for Statistical Computing, 2021. https://www.r-project.org/.
Rahman, M., Islam, M., Bräuning, A., 2018. Tree radial growth is projected to decline in south Asian moist forest trees under climate change. Glob. Planet. Chang. 170, 106–119. https://doi.org/10.1016/j.gloplacha.2018.08.008.
Rahman, M., Islam, M., Gebrekirstos, A., Bräuning, A., 2020. Disentangling the effects of atmospheric CO_2 and climate on intrinsic water-use efficiency in South Asian tropical moist forest trees. Tree Physiol. 40 (7), 904–916. https://doi.org/10.1093/treephys/tpaa043.
Raschka, S., 2020. Model Evaluation, Model Selection, and Algorithm Selection in Machine Learning (arXiv:1811.12808). arXiv. https://doi.org/10.48550/arXiv.1811.12808.
Rossi, S., Deslauriers, A., Griçar, J., Seo, J.-W., Rathgeber, C.B., Anfodillo, T., Morin, H., Levanic, T., Oven, P., Jalkanen, R., 2008. Critical temperatures for xylogenesis in conifers of cold climates. Glob. Ecol. Biogeogr. 17 (6), 696–707. https://doi.org/10.1111/j.1466-8238.2008.00417.x.
RStudio | Open source & professional software for data science teams. (n.d.). Retrieved April 10, 2022, from https://www.rstudio.com/.
Ruiz-Benito, P., Madrigal-González, J., Young, S., Mercatoris, P., Cavin, L., Huang, T.-J., Chen, J.-C., Jump, A.S., 2015. Climatic stress during stand development alters the sign and magnitude of age-related growth responses in a subtropical mountain pine. PLoS One 10 (5), e0126581. https://doi.org/10.1371/journal.pone.0126581.
Ryan, M.G., Phillips, N., Bond, B.J., 2006. The hydraulic limitation hypothesis revisited. Plant Cell Environ. 29 (3), 367–381. https://doi.org/10.1111/j.1365-3040.2005.01478.x.
Sabin, T.P., Krishnan, R., Vellore, R., Priya, P., Borgaonkar, H.P., Singh, B.B., Sagar, A., 2020. Climate change over the Himalayas. In: Krishnan, R., Sanjay, J., Gnanaseelan, C., Mujumdar, M., Kulkarni, A., Chakraborty, S. (Eds.), Assessment of Climate Change Over the Indian Region: A Report of the Ministry of Earth Sciences (MoES), Government of India. Springer, pp. 207–222. https://doi.org/10.1007/978-981-15-4327-2_11.
Salunke, P., Jain, S., Mishra, S.K., 2019. Performance of the CMIP5 models in the simulation of the Himalaya-Tibetan Plateau monsoon. Theor. Appl. Climatol. 137 (1), 909–928. https://doi.org/10.1007/s00704-018-2644-9.
Sánchez-Salguero, R., Camarero, J.J., Hevia, A., Madrigal-González, J., Linares, J.C., Ballesteros-Canovas, J.A., Sánchez-Miranda, A., Alfaro-Sánchez, R., Sangüesa-Barreda, G., Galván, J.D., Gutiérrez, E., Génova, M., Rigling, A., 2015. What drives growth of Scots pine in continental Mediterranean climates: drought, low temperatures or both? Agric. For. Meteorol. 206, 151–162. https://doi.org/10.1016/j.agrformet.2015.03.004.
Sánchez-Salguero, R., Camarero, J.J., Carrer, M., Gutiérrez, E., Alla, A.Q., Andreu-Hayles, L., Hevia, A., Koutavas, A., Martínez-Sancho, E., Nola, P., Papadopoulos, A., Pasho, E., Toromani, E., Carreira, J.A., Linares, J.C., 2017a. Climate extremes and predicted warming threaten Mediterranean Holocene firs forests refugia. Proc. Natl. Acad. Sci. 114 (47), E10142–E10150. https://doi.org/10.1073/pnas.1708109114.
Sánchez-Salguero, R., Camarero, J.J., Gutiérrez, E., González Rouco, F., Gazol, A., Sangüesa-Barreda, G., Andreu-Hayles, L., Linares, J.C., Seftigen, K., 2017b. Assessing forest vulnerability to climate warming using a process-based model of tree growth: bad prospects for rear-edges. Glob. Chang. Biol. 23 (7), 2705–2719. https://doi.org/10.1111/gcb.13541.
Sharma, E., Molden, D., Rahman, A., Khatiwada, Y.R., Zhang, L., Singh, S.P., Yao, T., Wester, P., 2019. Introduction to the Hindu Kush Himalaya assessment. In: Wester, P., Mishra, A., Mukherji, A., Shrestha, A.B. (Eds.), The Hindu Kush Himalaya Assessment: Mountains, Climate Change, Sustainability and People. Springer International Publishing, pp. 1–16. https://doi.org/10.1007/978-3-319-92288-1_1.
Shekhar, M., Bhattacharyya, A., 2015. Reconstruction of january–april discharge of Zemu Chuu–a first stage of Teesta River North Sikkim eastern Himalaya based on tree-ring data of fir. J. Hydrol. Reg. Stud. 4, 776–786.
Shekhar, M., Bhardwaj, A., Singh, S., Ranhotra, P.S., Bhattacharyya, A., Pal, A.K., Roy, I., Martín-Torres, F.J., Zorzano, M.-P., 2017. Himalayan glaciers experienced significant mass loss during later phases of little ice age. Sci. Rep. 7 (1), 10305. https://doi.org/10.1038/s41598-017-09212-2.
Shi, C., Gao, C., Zhang, Y., Shi, F., Shen, M., Shi, S., 2021a. The majority of tree growth on the monsoonal Tibetan Plateau has benefited from recent summer warming. CATENA 207, 105649. https://doi.org/10.1016/j.catena.2021.105649.
Shi, S., Liu, G., Li, Z., Ye, X., 2021b. Elevation-dependent growth trends of forests as affected by climate warming in the southeastern Tibetan Plateau. For. Ecol. Manag. 498, 119551. https://doi.org/10.1016/j.foreco.2021.119551.
Singh, J., Yadav, R.R., 2005. Spring precipitation variations over the western Himalaya, India, since A.D. 1731 as deduced from tree rings. J. Geophys. Res. Atmos. 110 (D1). https://doi.org/10.1029/2004JD004855.
Singh, S.P., Zobel, D.B., 2025. Pine-oak type: a unique resilient global system with high potential for nature-based solutions. Ecol. Indic. 175, 113536.
Singh, S.P., Singh, R.D., Gumber, S.U.R.A.B.H.I., Bhatt, S.P.A.R.S.H., 2017. Two principal precipitation regimes in Himalayas and their influence on tree distribution. Trop. Ecol. 58 (4), 679–691.
St. George, S., 2014. An overview of tree-ring width records across the northern hemisphere. Quat. Sci. Rev. 95, 132–150. https://doi.org/10.1016/j.quascirev.2014.04.029.
Stephenson, N.L., Das, A.J., Condit, R., Russo, S.E., Baker, P.J., Beckman, N.G., Coomes, D.A., Lines, E.R., Morris, W.K., Rüger, N., Álvarez, E., Blundo, C., Bunyavejchewin, S., Chuyong, G., Davies, S.J., Duque, Á., Ewango, C.N., Flores, O., Franklin, J.F., Zavala, M.A., 2014. Rate of tree carbon accumulation increases continuously with tree size. Nature 507 (7490), 90–93. https://doi.org/10.1038/nature12914.
Taylor, K.E., Stouffer, R.J., Meehl, G.A., 2012. An overview of CMIP5 and the experiment design. Bull. Am. Meteorol. Soc. https://doi.org/10.1175/BAMS-D-11-00094.1.
Telwala, Yasmeen, Brook, Barry W., Manish, Kumar, Pandit, Maharaj K., 2013. Climate-induced elevational range shifts and increase in plant species richness in a Himalayan biodiversity epicentre. PloS One 8 (2), e57103.
Thakur, S., Dhyani, R., Negi, V.S., Patley, M.K., Rawal, R.S., Bhatt, I.D., Yadava, A.K., 2021. Spatial forest vulnerability profile of major forest types in Indian Western Himalaya. For. Ecol. Manag. 497, 119527. https://doi.org/10.1016/j.foreco.2021.119527.
Tolwinski-Ward, S.E., Evans, M.N., Hughes, M.K., Anchukaitis, K.J., 2011. An efficient forward model of the climate controls on interannual variation in tree-ring width. Clim. Dyn. 36 (11), 2419–2439. https://doi.org/10.1007/s00382-010-0945-5.
Willmott, C.J., Matsuura, K., 2005. Advantages of the mean absolute error (MAE) over the root mean square error (RMSE) in assessing average model performance. Clim. Res. 30 (1), 79–82. https://doi.org/10.3354/cr030079.
Wilmking, M., van der Maaten-Theunissen, M., van der Maaten, E., Scharnweber, T., Buras, A., Biermann, C., Gurskaya, M., Hallinger, M., Lange, J., Shetti, R., Smiljanic, M., Trouillier, M., 2020. Global assessment of relationships between climate and tree growth. Glob. Chang. Biol. 26 (6), 3212–3220. https://doi.org/10.1111/gcb.15057.
Xiao, S., Li, S.-F., Wang, X.-J., Chen, L., Su, T., 2022. Cedrus distribution change: past, present, and future. Ecol. Indic. 142, 109159. https://doi.org/10.1016/j.ecolind.2022.109159.
Yadav, R.R., Braeuning, A., Singh, J., 2011. Tree ring inferred summer temperature variations over the last millennium in western Himalaya, India. Clim. Dyn. 36 (7), 1545–1554. https://doi.org/10.1007/s00382-009-0719-0.
Yadav, R.R., Gupta, A.K., Kotlia, B.S., Singh, V., Misra, K.G., Yadava, A.K., Singh, A.K., 2017. Recent wetting and glacier expansion in the northwest Himalaya and Karakoram. Sci. Rep. 7 (1), 6139. https://doi.org/10.1038/s41598-017-06388-5.
Yanai, M., Li, C., Song, Z., 1992. Seasonal heating of the Tibetan Plateau and its effects on the evolution of the summer monsoon. J. Meteor. Soc. Jpn. 70, 319–351.

Zeng, Q., Rossi, S., Yang, B., 2018. Effects of age and size on xylem phenology in two conifers of northwestern China. Front. Plant Sci. 8, 2264. https://doi.org/10.3389/fpls.2017.02264.

Zhang, Q., Kong, D., Shi, P., Singh, V.P., Sun, P., 2018. Vegetation phenology on the Qinghai-Tibetan Plateau and its response to climate change (1982–2013). Agric. For. Meteorol. 248, 408–417. https://doi.org/10.1016/j.agrformet.2017.10.026.

Zheng, Z., Jin, L., Li, J., Chen, J., Zhang, X., Wang, Z., 2021. Moisture variation inferred from tree rings in north Central China and its links with the remote oceans. Sci. Rep. 11 (1), 16463.

Zheng, P., Wang, D., Jia, G., Yu, X., Liu, Z., Wang, Y., Zhang, Y., 2022. Variation in water supply leads to different responses of tree growth to warming. For. Ecosyst. 9, 100003. https://doi.org/10.1016/j.fecs.2022.100003.

Supplementary material

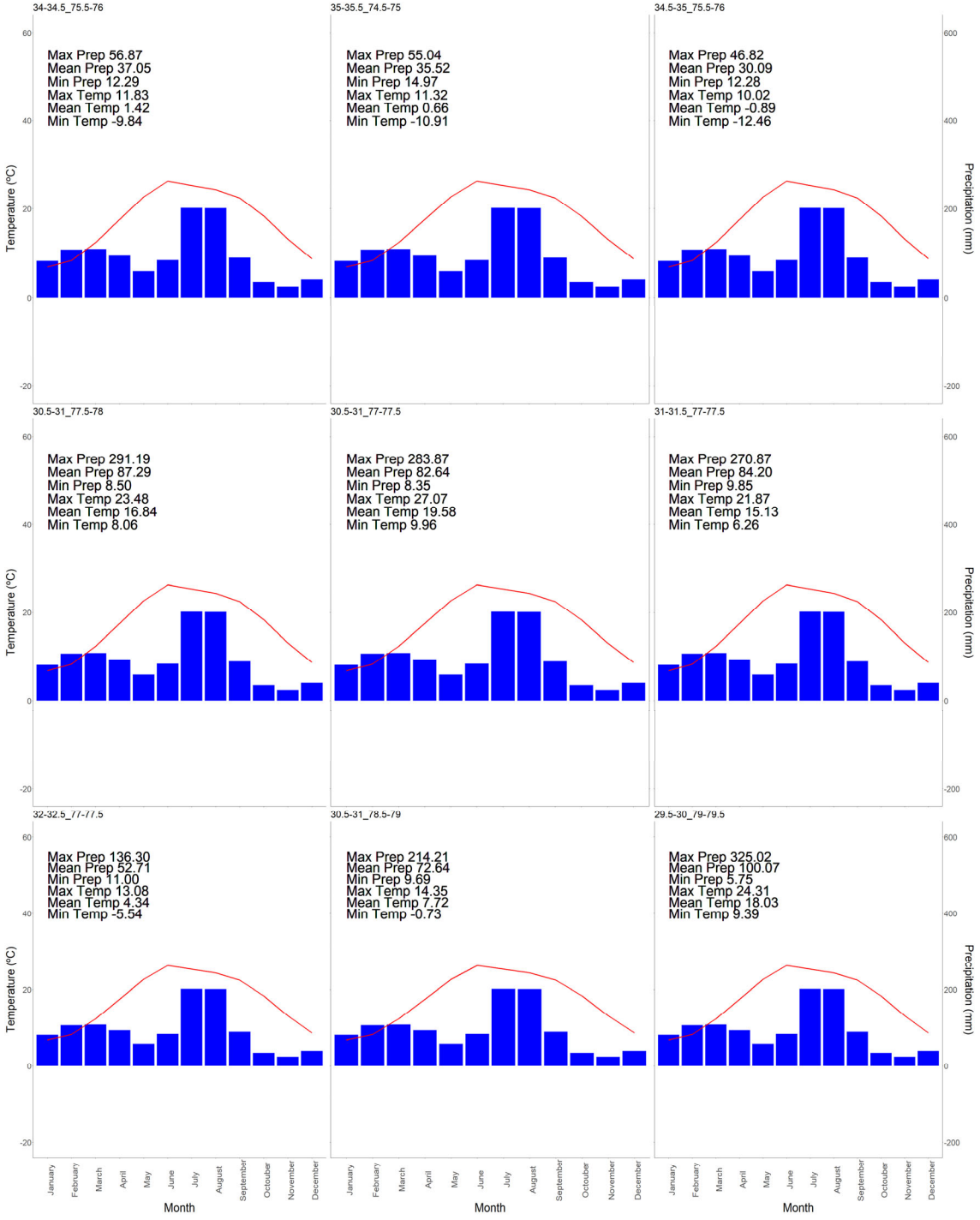

Figure S1: Climatic histogram for each cell studied with a resolution of 0.5º x 0.5º. Month represented in x axis while Temperature (ºC) is represented in y (left) axis via red line, precipitation (mm) is represented in the y (right) axis via columns. The title of each plot is the location represented, in the top right corner of each graph statistics are displayed (Max, Mean and Minimum values of precipitation and temperature)

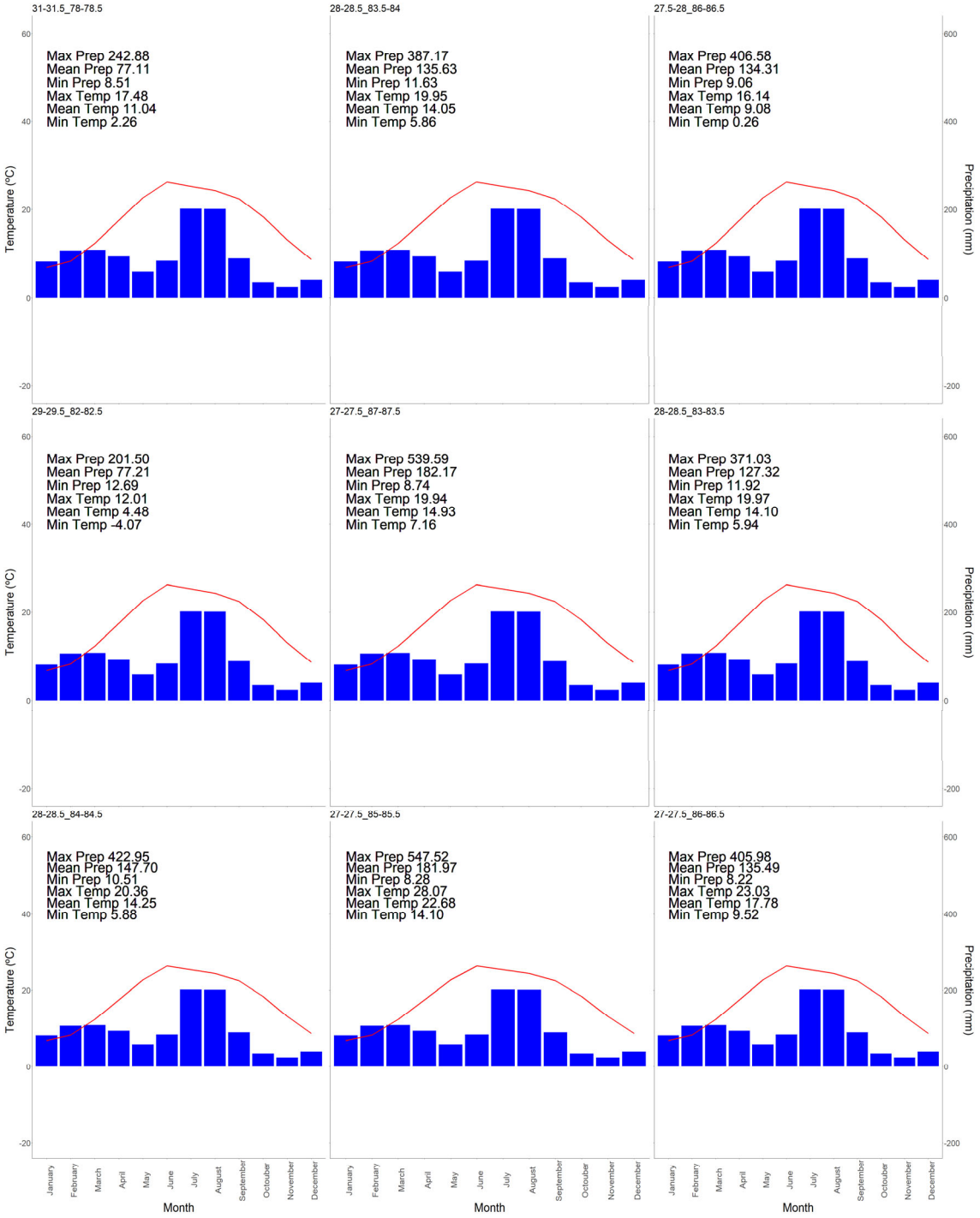

Figure S1 (cont): Climatic histogram for each cell studied with a resolution of 0.5º x 0.5º. Month represented in x axis while Temperature (ºC) is represented in y (left) axis via red line, precipitation (mm) is represented in the y (right) axis via columns. The title of each plot is the location represented, in the top right corner of each graph statistics are displayed (Max, Mean and Minimum values of precipitation and temperature)

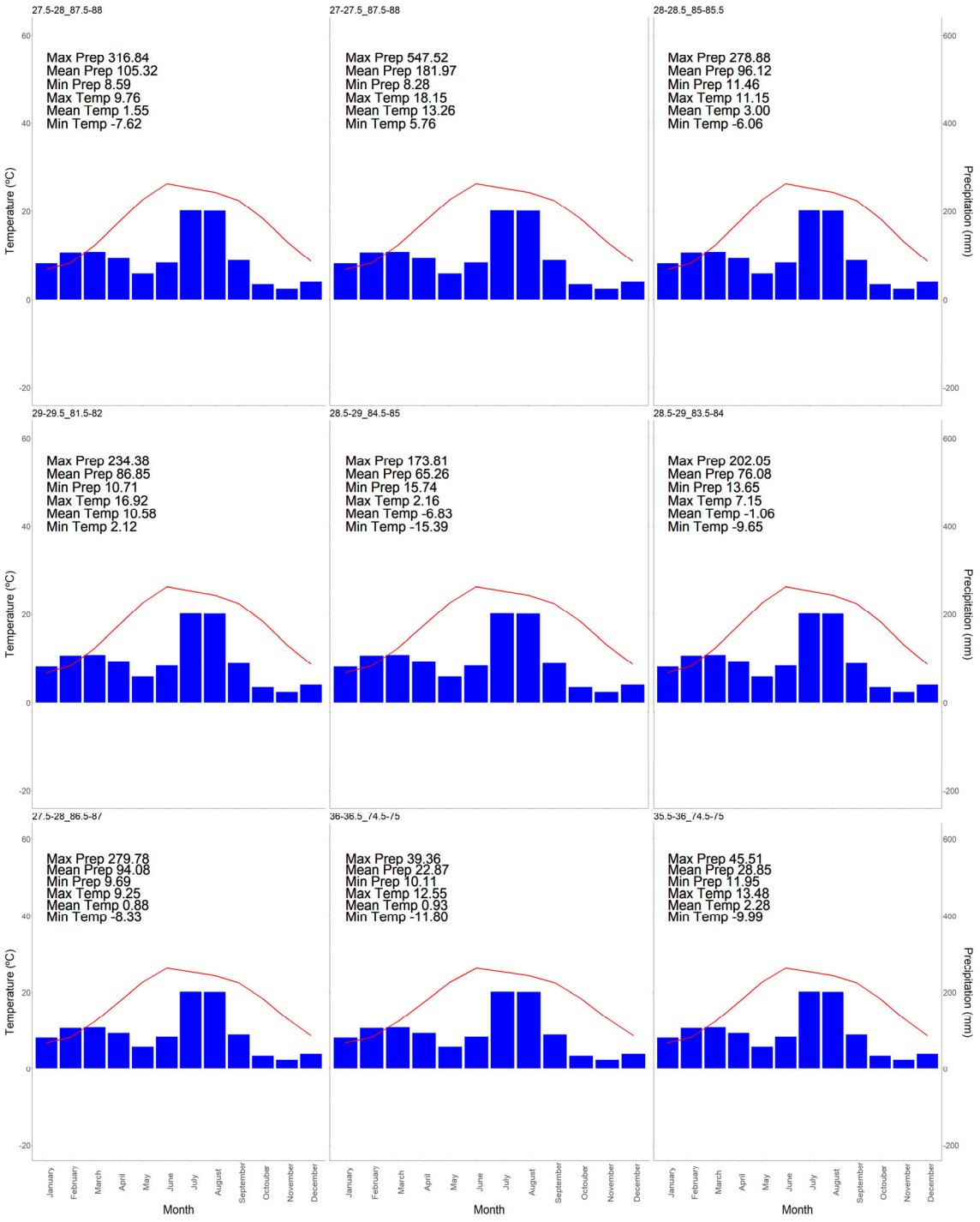

Figure S1 (cont): Climatic histogram for each cell studied with a resolution of 0.5º x 0.5º. Month represented in x axis while Temperature (ºC) is represented in y (left) axis via red line, precipitation (mm) is represented in the y (right) axis via columns. The title of each plot is the location represented, in the top right corner of each graph statistics are displayed (Max, Mean and Minimum values of precipitation and temperature)

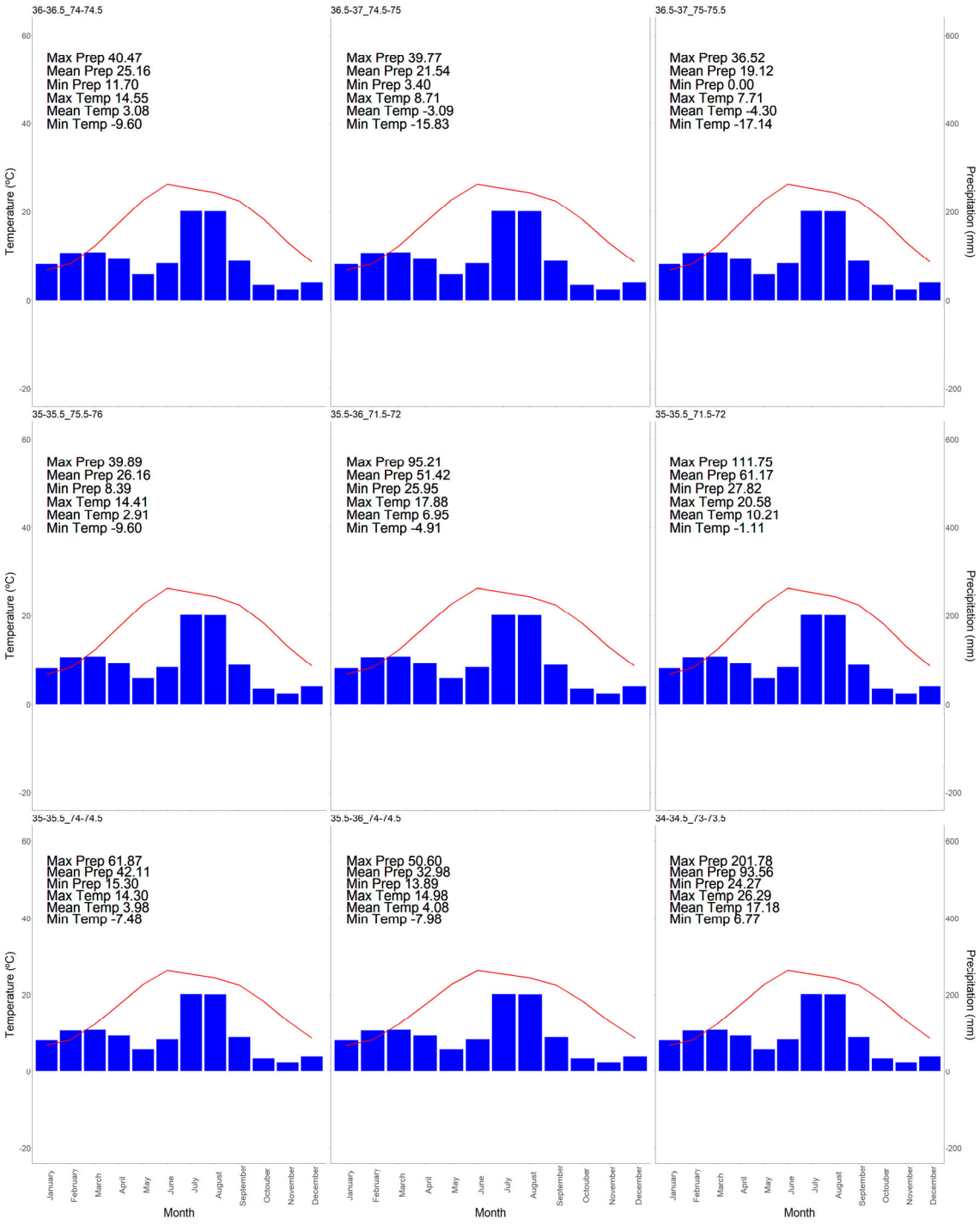

Figure S1 (cont): Climatic histogram for each cell studied with a resolution of 0.5º x 0.5º. Month represented in x axis while Temperature (ºC) is represented in y (left) axis via red line, precipitation (mm) is represented in the y (right) axis via columns. The title of each plot is the location represented, in the top right corner of each graph statistics are displayed (Max, Mean and Minimum values of precipitation and temperature)

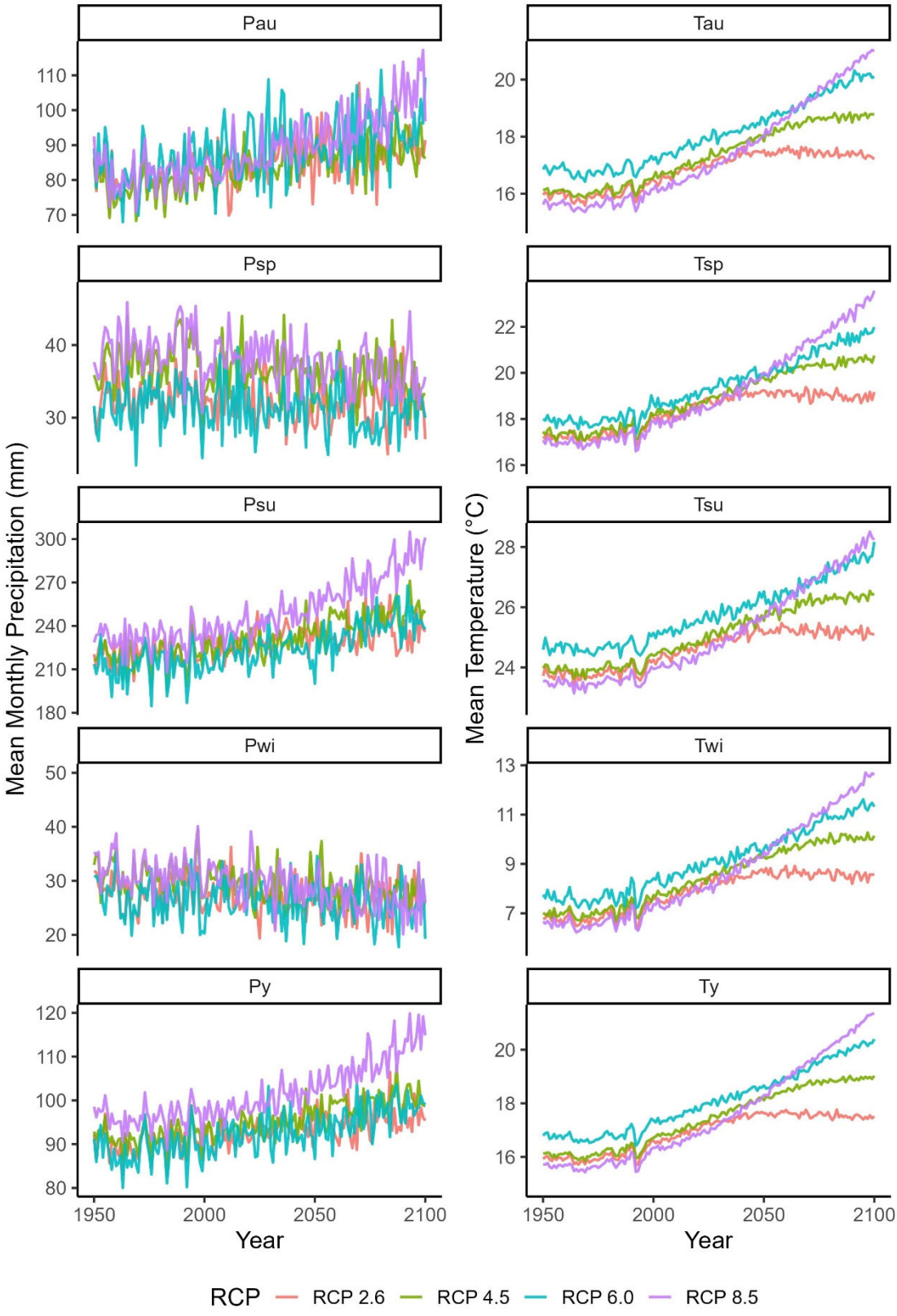

Figure S2. Future climatic models (RCP26-RCP45-RCP60-RCP80) for the Eastern region. Precipitation (mm) graphs are represented in the left column and Temperature (ºC) in the right column. Each graph is composed by the values of seasonal Precipitation or Temperature (y-axis) and year of study (x-axis).

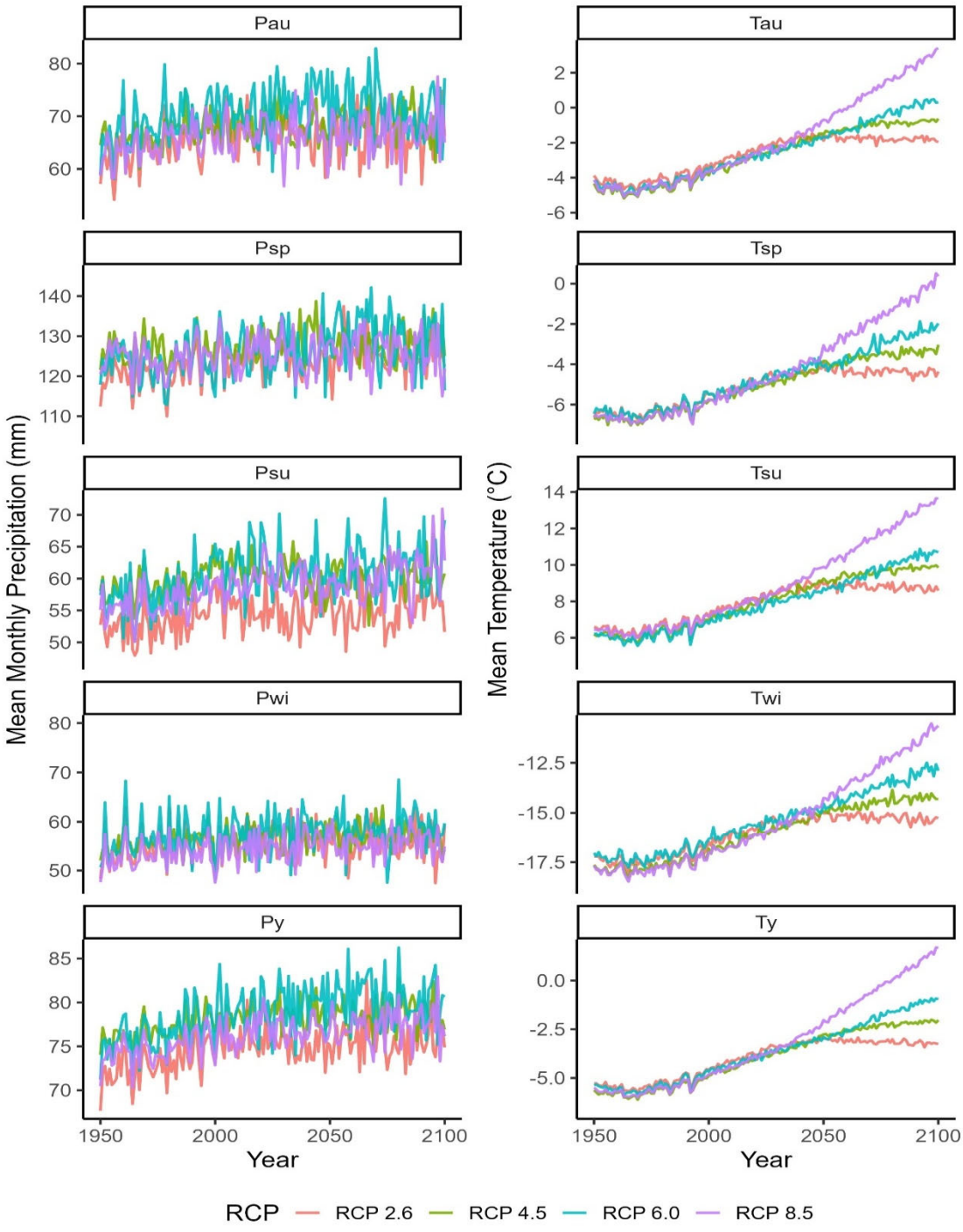

Figure S3. Future climatic models (RCP26-RCP45-RCP60-RCP80) for the Western region. Precipitation (mm) graphs are represented in the left column and Temperature (ºC) in the right column. Each graph is composed by the values of seasonal Precipitation or Temperature (y-axis) and year of study (x-axis).

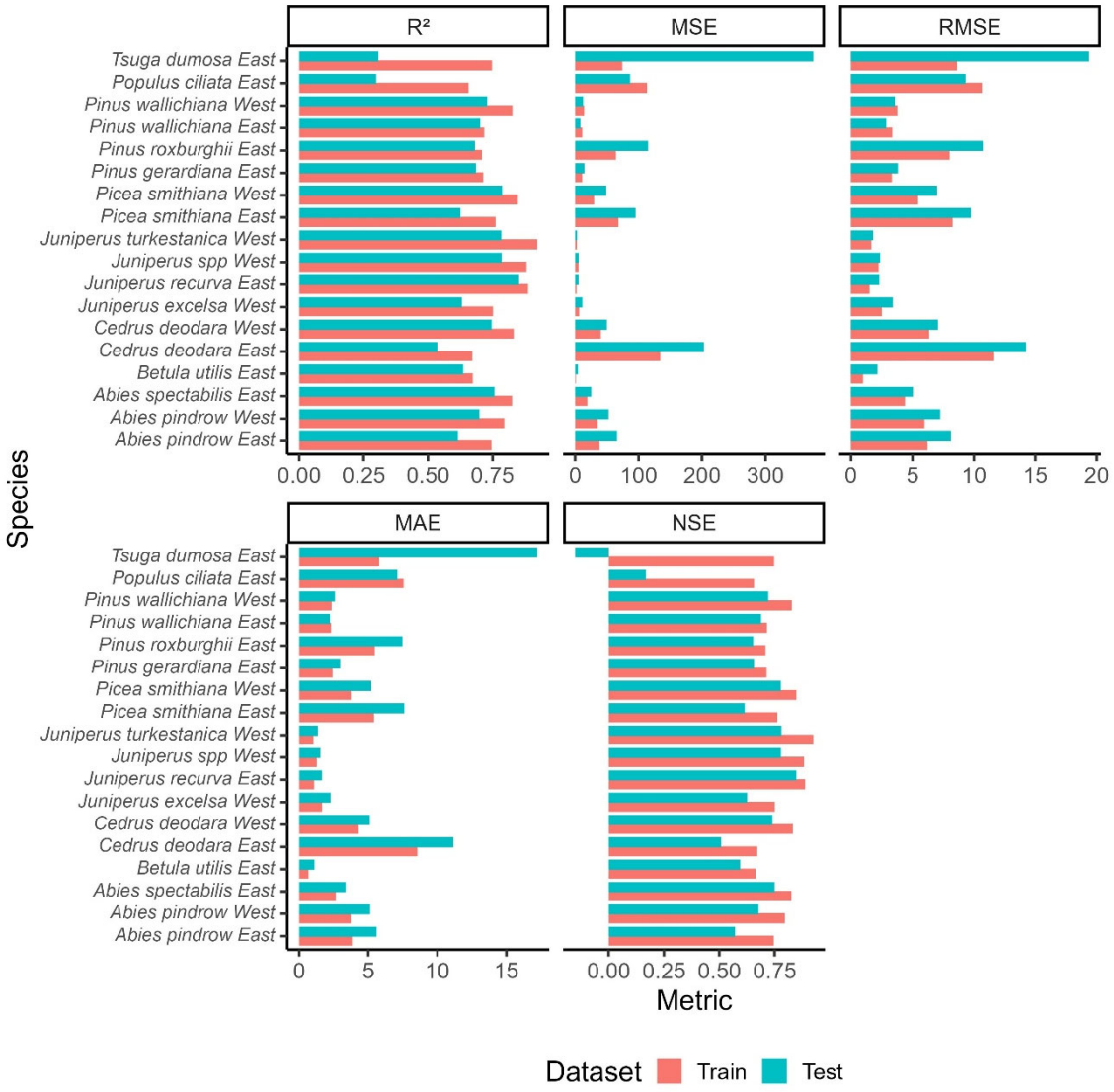

Figure S4. Comparison of training and testing performance metrics: R^2, RMSE, MAE, and NSE across species. Metrics are visualized in separate facets, with training and testing values represented as grouped bars for each species.

Table S1. Mean seasonal climatic values for each of the RCP scenarios studied (RCP26- RCP45- RCP60-RCP80) and each of the regions studied (E, Eastern region; W, Western region, respectively).

Seasonal	E26	E45	E60	E80	W26	W45	W60	W80
Taup	16.21	16.22	16.22	16.23	16.23	16.24	16.24	16.25
Twi	7.58	7.58	7.59	7.60	7.60	7.61	7.61	7.61
Tsp	16.75	16.76	16.76	16.77	16.77	16.78	16.78	16.78
Tsu	22.05	22.06	22.07	22.07	22.08	22.08	22.09	22.09
Tau	16.21	16.22	16.23	16.23	16.24	16.24	16.24	16.25
Paup	187.22	187.26	187.20	187.36	187.45	187.66	187.79	187.91
Pwi	65.52	65.54	65.53	65.49	65.37	65.31	65.25	65.40
Psp	152.77	152.45	152.53	152.54	152.66	152.45	152.67	152.79
Psu	565.59	565.77	565.91	566.36	566.63	566.82	566.84	566.34
Pau	183.97	183.92	184.08	184.16	184.37	184.50	184.61	184.82

Table S2. Variance explained (%) by age-effect, climate sensitivity model, autocorrelation model, and final fit of BAI model for each species in the Eastern (left) and Western (right) regions.

	Eastern				Western			
Species	Age	Climate	BAIp	Final	Age	Climate	BAIp	Final
Abies pindrow	0	53.37	21.78	75.16	2.51	54.54	22.32	79.37
Abies spectabilis	2.65	55.51	24.07	82.23	N/A	N/A	N/A	N/A
Betula utilis	13.12	36.17	19.32	68.62	N/A	N/A	N/A	N/A
Cedrus deodara	4.35	36.37	26.02	66.73	4.54	59.4	18.66	82.61
Juniperus recurva	6.23	63.17	19.45	88.85	N/A	N/A	N/A	N/A
Juniperus spp	N/A	N/A	N/A	N/A	1.17	66.99	19.41	87.58
Juniperus turkestanica	N/A	N/A	N/A	N/A	0.12	76.41	15.31	91.85
Juniperus excelsa	N/A	N/A	N/A	N/A	0.61	43.98	29.6	74.2
Picea smithiana	0.44	46.07	29.3	75.82	3.07	66	16.61	85.68
Pinus gerardiana	N/A	N/A	N/A	N/A	2.25	54.05	16.48	72.78
Pinus roxburghii	3.58	43.16	25.23	71.96	N/A	N/A	N/A	N/A
Pinus wallichiana	3.46	51.91	16.7	72.07	10.46	53.16	19.05	82.67
Populas ciliata	13.4	39.21	12.96	65.57	N/A	N/A	N/A	N/A
Tsuga dumosa	0.19	46.83	28.98	76	N/A	N/A	N/A	N/A

Table S3: ANOVA table on the relationship between Eastern and Western climate data for the period 1901-2020. The table contains the values of Degrees of Freedom (DF), Sum of Squares (Sum Sq), Mean of Squares (Mean sq), F Value (F Value) and Pr(>F). Significance codes 0 '***' 0.001 '**' 0.01 '*' 0.05 '.' 0.1 ' ' 1.

	Df	Sum Sq	Mean Sq	F value	Pr(>F)	
Taup	1	16.45	16.451	135.8	<2e-16	***
Residuals	116	14.05	0.121			

	Df	Sum Sq	Mean Sq	F value	Pr(>F)	
Twi	1	23.86	23.862	111	<2e-16	***
Residuals	116	24.94	0.215			

	Df	Sum Sq	Mean Sq	F value	Pr(>F)	
Tsp	1	35.23	35.23	129.6	<2e-16	***
Residuals	116	31.52	0.27			

	Df	Sum Sq	Mean Sq	F value	Pr(>F)	
Tsu	1	0.578	0.5778	4.565	0.0347	*
Residuals	116	14.683	0.1266			

	Df	Sum Sq	Mean Sq	F value	Pr(>F)	
Tau	1	16.98	16.981	138	<2e-16	***
Residuals	116	14.27	0.123			

	Df	Sum Sq	Mean Sq	F value	Pr(>F)	
Ty	1	12.52	12.52	202.1	<2e-16	***
Residuals	116	7.188	0.062			

Table S4: ANOVA table on the relationship between RCP models for Eastern and Western regions. The table contains the values of Degrees of Freedom (DF), Sum of Squares (Sum Sq), Mean of Squares (Mean sq), F Value (F Value) and Pr(>F). Signifiance codes 0 '***' 0.001 '**' 0.01 '*' 0.05 '.' 0.1 ' ' 1.

E26Taup	Df	Sum Sq	Mean sq	F value	Pr(>F)	
E80$Taup	1	101.31	101.31	7882	<2e-16	***
W26$Taup	1	25.39	25.39	1976	<2e-16	***
Residuals	236	3.03	0.01			

E45$Twi	Df	Sum Sq	Mean sq	F value	Pr(>F)	
E80$Twi	1	162.32	162.32	6985	<2e-16	***
W26$Twi	1	37.71	37.71	1623	<2e-16	***
Residuals	236	5.48	0.02			

E60$Tsp	Df	Sum Sq	Mean sq	F value	Pr(>F)	
E80$Tsp	1	166.33	166.33	7445	<2e-16	***
W26$Tsp	1	42.8	42.8	1916	<2e-16	***
Residuals	236	5.27	0.02			

E85$Tsu	Df	Sum Sq	Mean sq	F value	Pr(>F)	
E80$Tsu	1	93.83	93.83	3488.9	<2e-16	***
W26$Tsu	1	18.12	18.12	673.7	<2e-16	***
Residuals	236	6.35	0.03			

E26$Tau	Df	Sum Sq	Mean sq	F value	Pr(>F)	
E80$Tau	1	100.66	100.66	7773	<2e-16	***
W26$Tau	1	26.09	26.09	2015	<2e-16	***
Residuals	236	3.06	0.01			